AIRWAY SMOOTH MUSCLE ORIENTATION USING EN-FACE DISSECTION

MIN LEI

Department of Pathology
McGill University
Montreal, Canada.

March 1995

A thesis submitted to the Faculty of
Graduate Studies and Research
in partial fulfilment of the requirements of the degree of
Master of Science

ISBN 0-612-05582-5

Canada

ABSTRACT

Airway smooth muscle (ASM) shortening is the key event leading to broncho-constriction. The degree of airway narrowing which occurs with ASM shortening is a function both of the mechanical properties of the airway wall as well as the angle of orientation of ASM. If ASM is oriented very obliquely, ASM shortening would in part be transduced to a change in airway length rather than airway narrowing. Previous reports have suggested that the angle of ASM orientation may be as high as 30°. To measure ASM orientation we have developed a technique based on en-face dissection. The lungs from 4 cats and one human were fixed with 10% buffered formalin at 25 cmH_20 for 48 hrs. The airway generations 4 to 17 were dissected out from the left lower lobes. Each airway generation was individually embedded in paraffin from which 5μm thick serial sections were cut parallel to the airway long axis ("en-face") and stained with haematoxylin-phloxine-saffron. Each block yielded 3-5 sections in which the orientation of ASM nuclei relative to the airway long axis (θ) was measured as an index of ASM orientation. θ was measured clockwise and counterclockwise to the short axis by using a digitizing tablet and a light microscope (X250) equipped with a drawing tube attachment. Inspection of the sections revealed extensive ASM crisscrossing without a homogeneous orientation. Between 29 and 102 nuclei were measured per generation. Although there was considerable variation within airway generations, θ clustered between −20° and 10° in all generations and did not vary significantly between generations in any of the subjects. When θ was converted to an acute angle without regard to sign(Θ), the mean angle was 12–13° both in cat and the human lung. Based on current models of the influence of ASM orientation on constriction, a mean angle of 13° would not be expected to result in significant change in airway length.

ABRÉGÉ

La contraction et le rétrécissement du muscle lisse d'une voie aérienne (MLVA) est l'évènement pricipal qui engendre la bronchoconstriction. Le degré de rétrécissement d'une voie aérienne lors de la contraction du muscle lisse dépend des propriétés mécaniques de la voie aérienne ainsi que de l'angle d'orientation du muscle lisse. Si le muscle lisse a une orientation très oblique, le rétrécissement du MLVA engendrera plutôt un changement de la longueur de la voie aérienne qu'une diminution de la lumière de celle-ci. Des études antérieures ont suggéré que l'angle d'orientation des MLVA pouvait être aussi grande que 30°. Pour mesurer l'orientation du MLVA par rapport à la voie aérienne nous avons mis au point une technique se servant de la dissection "en-face". Les poumons de 4 chats et d'un être humain furent fixés dans la formaline à une pression de 25 cmH_20 pour 48 heures. Nous avons par la suite disséqué les générations 4 à 17 des voies aériennes des lobes inférieur gauche. Chaque génération fut préparé individuellement dans la paraffine puis des sections sériées de 5 microns coupés parallèlement à l'axe longitudinal des voies aériennes (en-face) et colorés par la technique hématoxilline-phloxine-safran. Chaque préparation nous a fourni 3 à 5 sections pour ainsi calculer l'angle d'orientation du noyau du muscle lisse par rapport à l'axe longitudinale de la voie aérienne (θ). Cet angle est donc un index d'orientation du MLVA. θ fut mesuré au microscope optique (X250) en utilisant une tablette permettant la digitalisation équipée d'un raccord en tube graphique. L'angle fut mesuré dans le sens des aiguilles d'une montre ainsi que dans le sens inverse par rapport à l'axe court de la voie aérienne. Nous avons mesuré entre 29 et 102 noyaux pour chaque génération de voie aérienne. L'analyse de sections sériées montra une distribution inhomogène de multiples croisements entre les fibres musculaires lisses. Bien qu'il y eut une certaine variation de l'angle (θ) entre les différentes générations de voies aériennes, cet angle se tenait entre -20 et 10° sans différence signifcative à l'intérieur d'un même poumon. En convertissant l'angle à un angle aigu sans tenir compte du signe (Θ), l'angle moyen était de 12-13° et chez les chats et chez l'homme. En tenant compte de modèles mathématiques sur l'influence de l'orientation du muscle lisse sur le rétrécissement d'une

voie aérienne lors d'une contraction, un angle moyen de 13° ne devrait pas affecter la longueur d'une voie aérienne.

ACKNOWLEDGMENTS

I am most grateful to my research director and thesis supervisor, Dr. David H. Eidelman, for his valuable guidance and thoughtful comments.

My deepest gratitude is also expressed to my other supervisor Dr. Moy Fong Chen, for her unhesitating help and constant inspiration.

Special indebtedness is owed to Dr. Héberto R. Ghezzo for his generous and timely assistance in mathematics and statistics; to my colleagues Ms. Carrie Dolman for technical assistance and for the tests of reproducibility; to Dr. Chonggang Wang for his support in laboratory work; and to Dr. Paulo Renzi for his French translation of the abstract.

Sincere thanks go to Dr. E. A. Zorychta, Director of Graduate Studies in the Department of Pathology, for her conscientious advice related to my program and her continuous encouragement.

This work would not have been possible without support from MRC Canada, QTS, and the JT Costello Memorial Fund.

TABLE OF CONTENTS

LIST OF FIGURES

LIST OF TABLES

ABBREVIATIONS

θ	Angle
2-D	Two dimension
3-D	Three dimension
ASM	Airway smooth muscle
ATS	American thoracic society
BRH	Bronchial hyperresponsiveness
Ca_i	Intracellular calcium
ECF-A	Eosinophil chemotactic factor of anaphylaxis
ECP	Eosinophil cationic protein
FcR1	Fc epsilon receptors
FEV_1	Forced expired volume in one second
FRC	Functional residual capacity
FVC	Forced expiratory vital capacity
HMW	High molecular weight
HPS	Haematoxylin phloxine saffron
IC	Inspiratory capacity
IP_3	Inositol trisphosphate
IRV	Inspiratory reserve volume
L	Length
L_o	Optimal length
LTB_4	Leukotrienes B_4
MBP	Major basic protein
MLC_{20}	20 kD light chain subunit of smooth muscle myosin
MLCK	Myosin light chain kinase
NANC	Non-adrenaline non-cholinergic
NCF	neutrophil chemotactic factor
NO	Nitric oxide
PAF	Platelet activating factor
PD_{20}	A fall of 20% in FEV_1
PGE_2	Prostaglandins E_2
P_o	Maximum active tension (maximum force)
Q-Q Plot	'Quantile-Quantile Plot'
RV	Residual volume
SD	Standard deviation
VC	Vital capacity
V_{max}	Maximum shortening velocity
W	Width
Δl_{max}	Maximum shorting capacity

BRIEF AIM OF STUDY

The purpose of this study was to develop a convenient method to measure airway smooth muscle (ASM) orientation around the airway wall in different airway generations, and to apply this method to the measurement of airway smooth muscle orientation as a function of airway generation in feline and human lungs.

The characteristic feature of asthma is excessive airway narrowing in response to nonspecific and specific stimuli (Moreno et al. 1986). Airway smooth muscle is believed to play a major role in determining bronchoconstriction in asthma. There is evidence to suggest that asthma is associated with increased airway smooth muscle quantity, likely due to both hyperplasia and hypertrophy (Dunnill et al. 1969, Heard and Hossain 1973, James et al. 1989, Ebina et al. 1990_b). Less is known regarding the arrangement of airway smooth muscle within the airway wall. Recently, Bates and Martin (1990) have suggested that the bronchoconstrictive effect of airway smooth muscle shortening is fundamentally related to both the material properties of the airway wall, and to the way in which airway smooth muscle is arranged around the airway wall.

The goal of this thesis was to investigate a technique for the study of airway smooth muscle orientation with confidence and a minimum of effort. The method uses direct sampling of airway smooth muscle by dissection of the airway parallel to its long axis.

1. INTRODUCTION

1.1. The normal anatomical features of the airway

The airway tissue consists of the epithelium with its attendant secretory glands, cartilage, smooth muscle, bronchial vessels, and supporting connective tissue.

Airway tree

The human airway tree includes the trachea, the bronchi and the bronchioles. The trachea is approximately 10–12 cm long in adults. Its width is 13 to 22 mm. The trachea is kept constantly patent by 16 to 20 C-shaped cartilaginous rings embedded in its walls (Hayek 1960). The trachea divides into right and left main bronchi, which enter the right and left lung at the hila. Coursing downward and outward, the bronchi divide into lobar branches. The left lung has upper and lower lobes; the right has upper, middle, and lower lobes. Correspondingly, there are two lobar bronchi in the left and three in the right lung. The lobar bronchi in turn divide into segmental bronchi to the several bronchopulmonary segments in each lung. There are three segments in the right upper lobe, two in the middle lobe, and five in the lower lobe. In the left lung, there are five in the upper and five in the lower lobe. The segmental bronchi branch into subsegmental bronchi. Further along the airway, subsegmental bronchi bifurcate until the terminal bronchiole is reached (Miller 1937). Finally, respiratory bronchioles terminate by branching into two or more alveolar ducts (Fawcett 1986).

In contrast, the cat lung is pyramidal-shaped. The right lung comprises four lobes: cranial, middle, caudal, and accessory. The left lung has cranial and caudal lobes, but the cranial lobe is further divided into cranial and caudal parts by a substantially shallower and incomplete fissure (Rosenzweig 1993).

The cat trachea is held open by a series of C-shaped cartilage in the wall. The trachea ends in the cranial portion of the mediastinum by dividing into the right and left principal bronchi, their walls also supported by C-shaped cartilages. The bronchi

subdivide into secondary and tertiary bronchi with cartilage rings, but the bronchioles have no skeletal supports (Chisson and Booth 1982).

The cartilage

The walls of the trachea contain cartilage which serves to maintain lumen patency. Cartilage is arranged differently in the extrapulmonary airways (the trachea and main bronchi) compared to the intrapulmonary airways (Hayward and Reid 1952_a). Cartilage in trachea and main bronchi are present as C-shaped plates (Bloom and Fawcett 1975), confined to the anterior and lateral airway walls, leaving the posterior wall free of cartilage. Intrapulmonary airways are divided into bronchi and bronchioles by reference to cartilage distribution (Hayward and Reid 1952_b). The bronchial cartilage plates are tethered together by dense fibroelastic tissue arranged predominantly in a longitudinal direction (Fraser et al. 1988). Near the point of division they are held in continuity with one another by longitudinal bars or by fibrocartilage, so that cartilages having quite complicated shapes are found and the greater part of the bronchial wall can be cartilaginous. In the medium sized bronchi and their branches the quantity of the cartilage decreases; the irregularly formed pieces become progressively smaller. At the dividing point at the transition into the bronchioles the last cartilage of all is saddle-shaped (Hayek 1960). By definition, bronchi are air tubes lying proximal to the last plate of cartilage found along an airway; bronchioles are found distal to the bronchi, beyond the last plate of cartilage and proximal to the alveolar region of the lung (Hayward and Reid 1952_b).

Bronchial mucous glands

Bronchial mucous glands lie in the submucosa with their ducts penetrating the mucosa to empty into the lumen (Nagaishi 1972). In the trachea, they are abundant in the posterior wall and are found as well in the anterior and lateral walls. In the larger bronchi they are abundant. In the small bronchi, their number decreases, but they are absent in the bronchioles (Hayek 1960). The surface epithelium is always moist but in

healthly airways no mucus blanket is seen with the naked eye. Even when secretions are present, they do not form a blanket. Secretion is seen as a streak or clump and is discontinuous (Sturgess 1977).

Airway epithelium

The epithelium is pseudo-stratified consisting of a single layer of ciliated columnar cells interspersed with goblet cells (Miller 1937) and basal cells. These cells are gradually lost in the distal bronchi and bronchioles as the epithelium becomes columnar in appearance. Normally, the epithelial layer may act as a modulator of smooth muscle tone (Gao and Vanhoutte 1994) and as a chemical permeability barrier inhibiting movement of agonists from the lumen to the smooth muscle (Omari et al. 1993).

Basement membrane

The basement membrane is an approximately 5 μm thick (Bloom and Fawcett 1975) layer of specialized extracellular matrix that acts as a supporting structure on which epithelial cell grow (Laitinen and Laitinen 1994). It constitutes a boundary between the base of the epithelium and the lamina propria (Nagaishi 1972). It is an open-network structure through the pores of which are transmitted nerve fibres. Polymorpholeukocyte and other inflammatory cells may migrate through the basement membrane to the surface from the underlying connective tissues. Tissue fluid also passes freely through this structure to nourish the overlying epithelium passing into the intercellular canals between the epithelial cells. The basement membrane consists of a condensation of intercellular ground substance in which reticulin fibres are embedded (Spencer 1984). There is evidence that the basement membrane is better defined and thinner in small airways (Netter et al. 1979).

Beneath the basement membrane lies the loose lamina propria which normally contains a few lymphocytes, numerous mast cells and an occasional polymorpholeucocyte together with a rich capillary network surrounded by fine-beaded, non-myelinated nerve

fibres. The outermost part of the lamina propria consists of a fine sheet of longitudinal elastic tissue where it abuts on the muscle coat (Nagaishi 1972).

Elastic fibres

The elastic tissue in the trachea runs lengthwise along the bronchi and bronchioles between the muscular layer and the lamina propria (Nagaishi 1972). The smooth muscle coat is sandwiched between the elastic sheet forming the deep part of the lamina propria and an external sheet of elastic tissue on its outer surface (Spencer 1984). Miller (1937) reported that the elastic fibres in general follow a longitudinal course, but at the point where the branch leaves the main-stem bronchus they swing over to the opposite side of the bronchus and in that way they encircle the branch as it leaves the main-stem bronchus. In the sacculi alveolares and the alveoli, the elastic fibres form an intricate network. The elastic fibres surround the cartilage plates and are continuous with the connective tissue of the surrounding pulmonary tissue and with that accompanying the large vessels (Bloom and Fawcett 1975). There is some inter-species variation in the elastic fibres. Amiri and Gabella (1988) found that the longitudinal oriented elastic membrane in the trachea mucosa is thin in the cat and dog, thick and diffuse in cattle and sheep, but more compact in the goat.

1.2. Airway smooth muscle

1.2.1. Shape and size

The airway smooth muscle fibre is an elongated, slender cell (spindle-shaped) with tapering ends, containing a single cigar-shaped nucleus in the expanded central region of the cell. Smooth muscle cells lie approximately parallel to each other, forming bundles or sheets and very rarely branch. Smooth muscle cells vary in length in different organs, from 20 μm in small blood vessels to 500 or 600 μm in the pregnant uterus (Leeson 1976, Krause and Cutts 1981, Gabella 1973, 1981). In the muscularis external

smooth muscle cells are 2 to 4 μm in diameter (Gabella 1973). The length of the dog tracheal smooth muscle cell exceeds 100 μm and has a diameter of 3.3 ± 0.5 μm (SD) (Suzuki et al. 1976).

1.2.2. Fine structure

The contents of the smooth muscle cell include the cell membrane, caveolae, dense bands, sarcoplasmic reticulum, filaments, mitochondria and other organelles. The smooth muscle cell contains actin and myosin, and is packed with filaments of which three types have been described: thick, thin and intermediate (Gabella 1981). Heumann (1970) and Rice et al. (1970) have found areas of ordered hexagonal packing of thin filaments, with an 11–12 nm interfilament (centre–to–centre) spacing, but the precise packing of the thin and thick filaments is still uncertain. Filaments lie parallel to one another, and the thick filaments in transverse section often have an irregular profile. In many preparations, thin filaments are very regularly arranged and are grouped into bundles. They are circular in transverse section, have a smooth outline and form a fairly uniform population (Gabella 1981). The arrangement of the myosin molecules in the thick filaments of smooth muscle is probably different from that in skeletal muscles. Smooth muscle lacks the regular striated pattern of skeletal and cardiac muscle which is the result of the very regular arrangement of the contractile proteins, actin and myosin, and the structural Z–lines. Thick myosin filaments contain the same heavy chain proteins as skeletal muscle, but different light chains. Thin filaments contain the same actin and tropomyosin proteins as skeletal muscle, but no troponin (Hartshorne 1987). In intestinal smooth muscle, there is evidence that the contractile units are made up of small bundles of interdigitating thick and thin filaments that are irregularly shaped and randomly arranged. When the muscle contracts, the thick and thin filaments are thought to slide over each other (Ganong et al. 1979). In general, thick and thin filaments of smooth muscle cells are regarded as corresponding to myosin and actin filaments (Shoenberg and Needham 1976). However, it has been suggested that in smooth muscle, myosin is labile and aggregates into

filaments only prior to contraction (Krause and Cutts 1981). Stephens et al. (1988) has suggested that intermediate filaments may play the same role in asthma.

On the cell membrane, a large part of the smooth muscle cell surface is separated from that of neighbouring cells by a gap of 100 nm or more, in which collagen fibrils, elastic fibres and other extracellular material are present. Generally, airway smooth muscle is regarded as being the multi-unit type, where each cell is innervated and cell-to-cell communication is poor. This is because there are gap junctions which provide pathways of low resistance along which electrical signals can be transmitted (Rodger 1992, Barnes 1988). Other junctions normally present in airway smooth muscle are intermediate junctions; they may provide sites of mechanical attachment between cells and for the contractile proteins within cells (Daniel and O'Byrne 1991). Tight junctions do not occur between muscle cells (Tani et al. 1977).

1.2.3. Distribution along airway tree

Smooth muscle can be found from the trachea to the alveolar ducts (Bloom and Fawcett 1975, Wang 1988). The bundles of smooth muscle are inserted on the inner surface in between the lamina propria and submucosal glands. At light microscopic levels, there seems to be little difference in morphology between smooth muscle cells in the bronchioles, bronchi, and trachea. In human airways, differences are mainly in orientation and in numbers of cells present (Hayek 1960) at different levels. Horsfield (1974) reported that trachea and bronchi have relatively small amounts of muscle and that the majority of smooth muscle is located in bronchioles and alveolar ducts. In the terminal bronchioles, the ratio of muscle layer to total wall thickness is larger than in any of the other airways. A quantitative study demonstrated that the relative amount of smooth muscle increases from the trachea to the terminal bronchioles in normal human airways (Hogg 1980), so that when it is expressed as a percent of wall thickness, smooth muscle accounts for about 5% of the wall thickness in large airways and 20% of the wall thickness in bronchioles.

In the trachea, the thick muscle bundles are situated as a transverse sheet across the incomplete cartilaginous rings of the trachea (Stephens et al. 1980). In bronchi, Toldt (1888. *Lehrbuch der Gewebelehre. 3. Auf. Stuttgart.), as quoted in Miller (1937) observed* "the muscle is arranged in flat bundles which have, in general, a nearly transverse course and unite to form a network. Between these bundles there are spaces, bounded by acute angles, which are situated transverse to the long axis of the bronchi". In the small bronchi, muscle bundles are altered in that the thinner ones are arranged in crisscrossing helical turns (Hayek 1960), with fibres spiralling in both directions and crisscrossing in the walls (Murray 1986). Miller made a reconstruction model from a dog bronchiole and its subdivisions. He demonstrated the tendency of the muscle bands to have a more or less triangular arrangement at the place where branches are given off. This arrangement is quite characteristic and has probably a direct relationship to the arrangement of the elastic fibres. In the bronchioles, the screw-like turns are said to be somewhat steeper (Hayek 1960). Finally, smooth muscle forms knobs at the end of walls of adjacent alveolar sacs opening into the ducts (Macklin 1929). All of these observations were made qualitatively; quantitative information regarding smooth muscle orientation has not been readily available.

Airway smooth muscle has a similar architecture to that of other tubular organs but differs from that found in hollow organs (eg. uterus). Vascular smooth muscle is arranged in one or two circular or helical layers of the longitudinal axis (Rhodin 1980), which serves only to change the calibre of the lumen. In contrast, in the wall of the intestine, smooth muscle is arranged in separate longitudinal and circumferential layers. The coordinated action of these layers permits constrictions that move along the intestine as peristaltic waves, propelling the contents through the lumen. In other hollow organs, such as the bladder or uterus, the smooth muscle forms poorly defined layers of elaborately interlacing coarse bundles oriented in different directions (Bloom and Fawcett 1975).

1.2.4. Airway smooth muscle mechanics

Properties of ASM

Airway smooth muscle in general serves to sustain the profile of the airway wall. Although the physiologic role of airway smooth muscle is uncertain, there is data to support the notion that airway smooth muscle has some role in distribution of pulmonary ventilation; such as maintenance of perfusion homogeneity, reduction of anatomical dead space, stabilization of the airway during forced expiration, and opening of adjacent alveoli by bronchoconstriction (Williams 1981, Stephens 1987).

Contractile mechanisms of smooth muscle

There are striking similarities but also marked differences between skeletal and smooth muscle. Many of the differences can be related to the functions served by the two kinds of muscle. Skeletal muscle spans attachment points between different parts of the skeleton and individual motor units can be recruited to shorten and perform work (Stephens and Hoppin 1986). The efficiency of conversion of ATP into work is paramount. Smooth muscle has to alter organ dimensions in the absence of a skeleton and sustain tone for long periods (Gabella 1976). The economy of force maintenance is critical. Although the mechanism of smooth muscle shortening is uncertain so far, it is generally accepted that the sliding filament cross bridge mechanism is responsible for chemomechanical transduction in smooth muscle (Dillon et al. 1981), but that it is much less regularly organised than is striated muscle. Sarcomeres such as those visualized in skeletal muscle are not well seen in smooth muscle (Ganong 1991). Although the behaviour of smooth muscle from the standpoint of the mechanics of contraction is similar to skeletal muscle, smooth muscle is able to shorten to a greater extent than skeletal muscle.

In smooth muscle, contraction occurs when myoplasmic calcium concentrations increase above resting values. Calcium is the primary messenger of contractile activation. Cytoplasmic calcium concentrations can be altered by changes in surface membrane

potential (electromechanical coupling), and by membrane mediated mechanisms independent of changes in potential difference (pharmacomechanical coupling). Calcium can be made available from intracellular sources or from the outside through an increase in permeability mediated either by voltage or ligand-gated channels. Intracellular Ca^{2+} (Ca_i) concentration plays an important role in the regulation of contraction-relaxation in smooth muscle (van Breemen et al. 1980, Wong and Klassen 1993). Activation of a variety of cell surface receptors results in the catalyzed hydrolysis of phosphatidylinositol 4,5-biphosphate by phospholipase to form inositol 1,4,5-trisphosphate (IP_3) and diacylglycerol (DAG). IP_3 is recognized as an important second messenger that signals the release of intracellular calcium while DAG activates protein kinase C. IP_3 binds with a receptor on the sarcoplasmic reticulum or other calcium storing organelles to cause release. The mechanism by which a fall in intracellular calcium causes an increase in permeability to extracellular calcium is not clear. Recently, a model of calcium regulation in smooth muscle cells was studied by Wong and Klassen (1993). They propose that the intracellular Ca^{2+} store is comprised of two pools: The A-store which is sensitive to IP_3 and the C-store, insensitive to IP_3 but sensitive to Ca_i. The A-store is refilled by Ca^{2+} from the C-store and reuptake of Ca_i.

Ca^{2+} allows the myosin light chains to be phosphorylated by myosin light chain kinase; phosphorylation of the regulatory light chain of smooth muscle myosin by Ca^{2+}/calmodulin-dependent myosin light chain kinase increases actin-activated MgATPase activity and initiates smooth muscle contraction (Hartshorne 1987, Tang et al. 1992). This myosin light chain kinase consists of two subunits, and it is one of these subunits, calmodulin, which binds Ca^{2+} (Hartshorne 1987, Sparrow et al. 1984, Stephens 1992).

Length-tension relationships

Isometric studies of the relationship between force and tension or load and muscle length provide information about the ability of the muscle to stiffen and support loads (in

airways, this would correspond to maintenance of tone). The evidence shows that canine tracheal and bronchial smooth muscle have a length–tension relationship analogous to that of skeletal muscle (Stephens et al. 1968, Stephens and Kroeger 1980_b). Length–tension curves elicited by supramaximal electrical stimulation of isolated canine tracheal smooth muscle, and active tension developed during stimulation, increases with muscle length to reach a maximum then declines with further stretching (Stephens et al. 1969, Stephens and Kroeger 1980_b). The resting tension curve shows the nonlinear shape expected from complex biological tissue. Tension begins to develop at about 80% optimal length (L_o). Under normal *in vitro* conditions, resting tension at L_o is low (less than 10% of P_o. P_o=maximum active tension). Optimal length is the length at which the muscle develops maximal active tension, and P_o defines that tension. Smooth muscle can develop tension over a much wider range of length than skeletal muscle. A length change of tracheal smooth muscle, in excess of 25% of L_o, produces stress–relaxation that results in development of hysteresis; repeated cycling of tissue length narrows the loop (Stephens and Kroeger 1980_b). The maximal isometric tension developed at any length of tracheal smooth muscle is influenced by the history of the contraction. Another feature is the ability of this muscle to shorten much more than skeletal muscle. The latter can only shorten to 65% of L_o, whereas the former shortens in principal to 10%.

Force–velocity relationship

Recently, Wang et al. (1994) have reported the force–velocity relationship in canine airway smooth muscle is nonhyperbolic, and therefore different from skeletal muscle. Maximal shortening velocity (Vmax) in smooth muscle is also markedly less than in skeletal muscle. In skeletal muscle only one type of cross bridge is active through the time course of a contraction, but in smooth muscle evidence suggests two types of behaviour that have been identified. Normally cycling crosse bridges that are activated early in the contraction and slowly cycling or latch bridges (LBR) that are active later (Dillon et al. 1981).

1.3. Asthma

1.3.1. Definition of asthma

A useful working definition was proposed in 1962 by the American Thoracic Society as follows: "Asthma is a disease characterized by an increased responsiveness of the trachea and bronchi to a variety of stimuli and manifested by widespread narrowing of the airways that changes in severity either spontaneously or as a result of therapy" (ATS 1962).

1.3.2. Pathologic changes in asthma

The pathology of asthma has mainly been derived from study of autopsy specimens, particularly where asthma has been the cause of death, but occasionally from those dying from an incidental cause. Thus, the pathological material usually demonstrates the most severe effects of asthma, although these findings in different types (extrinsic and intrinsic) of asthma are said to be similar (Hogg 1985). James et al. (1989) found that the airway wall in asthmatic subjects is thicker than in normal subjects. They suggested that this thickness was accounted for by chronic inflammation and hypothesized that this thickening could be as important as smooth muscle shortening in determining the airway responsiveness. Morphological changes in asthma may include hypertrophy and hyperplasia of airway smooth muscle, loss of surface epithelium, goblet cell prominence or squamous metaplasia, apparent thickening of the basement membrane and with inflammatory infiltrate, enlarged mucous glands, partial occlusion of the lumen with mucus and cellular debris (airway mucous plugging), vascular congestion and exudation of fluid into the wall associated with inflammatory cell infiltration (Hogg 1985, Dunnill 1960, Fraser et al. 1994).

Smooth muscle

Airway smooth muscle contraction plays a central role in asthma. The extreme sensitivity of the airways to physical, chemical, and pharmacological stimuli is a

characteristic feature, and asthmatics develop a greater degree of bronchoconstriction in response to a wide variety of stimuli than do healthy subjects. Although much has been learned about neurohumoral control of airway smooth muscle in healthly and diseased airway, the fundamental cause is unknown (Workshop Report: 1985). Mechanically, airway smooth muscle itself may be the locus of the abnormal responses.

The pathologic changes in airways include muscle hypertrophy and constriction, particularly of the small airways (Turner-Warwick 1989). Dunnill and colleagues (1969) reported an increase in smooth muscle in the major bronchi of asthmatic subjects. Heard and Hossain (1973) by using a point-counting technique, have shown there is hypertrophy and hyperplasia of muscle in the segmental airway wall, and that the increased volume of muscle in asthma was the result of hyperplasia of muscle cells rather than hypertrophy. A more recent study demonstrated the presence of increased smooth muscle thickness also in the peripheral airways (Saetta et al. 1991).

Inflammatory cell infiltration

The most numerous and characteristic cell in the inflammatory infiltrate in asthma is the eosinophil. It is found in the airway lumen having migrated across either intact epithelium or basement membrane by diapedesis. Eosinophils can release a variety of mediators, including leukotriene C_4, PAF, oxygen radicals, and also polycationic proteins, such as major basic protein (MBP) and eosinophil cationic protein (ECP), which are toxic to the airway epithelial cells (Frigas and Gleich 1986, Coyle et al. 1993a & 1993b) and may contribute to hyperresponsiveness by directly altering smooth muscle function. Indeed, activated eosinophils in the airway lumen may thus lead to epithelial damage, which may increase the bronchial reactivity. More recently, it has been suggested that leukocyte integrin CD18 is involved in the recruitment of leukocytes to the airway, and may contribute to the accumulation of eosinophils in the airway lumen (Milne and Piper 1994).

Neutrophils migrate into bronchial tissue as a result of the release of mast cell-derived chemotactic factors, although neutrophils are not usually observed at autopsy after asthma deaths but are often seen in the bronchi of asthmatics who died from non-asthmatic causes (Kay 1985). Nevertheless, increased numbers of both neutrophils and eosinophils have been associated with the late asthmatic response in allergen challenge tests (Laitinen and Laitinen 1994). The number of lymphocytes are also increased in asthma. They could contribute to immunological mechanisms in asthma. Evidence suggests that asthma is associated with increased production of cytokines thought to be produced by T helper type 2 cells (TH2), CD4-positive ($CD4^+$) lymphocytes (Kay et al. 1991, Robinson et al. 1992).

Mast cells are also said to play a major role in the pathogenesis of allergic asthma (Newball and Lichtenstein 1981). Mast cells have Fc epsilon receptors (FcR1) on their membrane surface and these receptors have a high affinity for IgE molecules (Roitt et al 1989). Several chemical components are released during mast cell degranulation; such as histamine, ECF-A, high molecular weight (HMW) NCF, LTB_4, and PAF (Kay 1985). These mediators cause airway smooth muscle contraction, vascular leakage and inflammatory cell infiltration. They may increase and cause nonspecific airway hyperreactivity and both the early and late allergic airway responses (Kaliner 1989).

Mucus-secreting tissues

The bronchi and bronchioles exhibit mucosal and submucosal edema in asthma. There is hypertrophy of the submucosal glands and an increase in the number of goblet cells both in central airways and in small peripheral airways (Lopez-Vidriero et al. 1993), contributing to hypersecretion during an asthma attack. Fatal asthma is frequently accompanied by intraluminal mucous plugs which contribute to the decrease in airflow.

Airway epithelium

Airway epithelial damage is common to those disorders associated with hyperreactivity (Campbell et al. 1988). Histologic shedding and damage of airway surface epithelium is a prominent postmortem finding in asthma (Dunnill 1960, 1975, Montefort and Holgate 1993_a, Montefort et al. 1993_b), but bronchial biopsy specimens have revealed that it may occur even in subjects with mild asthma (Laitinen et al. 1985). Patchy epithelial damage may be produced by basic proteins derived from eosinophils, perhaps also by the release of oxygen radicals from various inflammatory cells, and possibly as a consequence of submucosal edema. Damaged epithelial cells may release proinflammatory mediators and expose nerve endings that can directly increase responsiveness of bronchial smooth muscle (Barnes 1987, 1989). Bronchial biopsies from living asthmatic subjects have revealed extensive epithelial disruption, with exposure of nerve endings regarded as afferent and presumably irritant (Laitinen et al. 1985).

In addition, the airway epithelium itself has effects on airway smooth muscle. Intact epithelium inhibits muscle tone by releasing prostaglandin E_2 (PGE_2). PGE_2 has direct inhibitory effects on the muscle and also acts by inhibiting vagal neural transmission (Jacoby et al. 1988). Human and canine airway epithelial cells in *vitro* produce low concentrations of PGE_2, but when they are stimulated by inflammatory mediators, these cells produce large amounts of PGE_2 which may have profound effects on smooth muscle (Barnett et al. 1987).

Basement membrane

Dunnill (1960), Dunnill et al. (1969) and Lamb (1990) reported that fatal asthma was associated with a 2-fold thickening of the basement membrane. Cutz et al. (1978) reported the basement membrane was normal in childhood asthma. Although the mechanism is poorly understood, pathologic studies have demonstrated that a thickened basement membrane includes collagens, fibronectin (Laitinen et al. 1989, Roche et al. 1989) and nucleated myofibroblasts. Brewster and colleagues (1990) confirmed these cells are not derived from the bronchial smooth muscle, and they proposed that bronchial

myofibroblasts are responsible for the characteristic subepithelial fibroses seen in allergic asthma.

Recently, the investigators finding suggested that the basement membrane not only provides mechanical support for epithelial cell growth but also influences cellular behaviour (Laitinen and Laitinen 1994).

1.3.3. Physiologic changes in asthma

In asthma attacks, the principal physiologic characteristic is airway obstruction and a marked increase in airway resistance (McFadden 1988). The increase in airway resistance is caused by contraction of bronchial smooth muscle and by luminal narrowing produced by a combination of mucosal edema and retention of secretions (Reed 1980). Patients have difficulty in moving the tidal air in and out. Although inspiratory resistance also rises, the abnormality is more pronounced during expiration, because of closure of the airways as the lung empties. At this point, further expiratory effort does not produce any increase in expiratory flow rate and may even intensify airway collapse.

The severity of the obstruction is reflected in the spirometric measurements of expiratory volume and airflow. The vital capacity (VC), forced expiratory vital capacity (FVC), inspiratory reserve volume (IRV) and inspiratory capacity (IC) are reduced during an acute attack (Reed 1980). With progressive obstruction, expiration becomes increas-ingly prolonged. Increases in RV and FRC occur. The effect of these events is alveolar hyperinflation, accompanied by an increased static lung volume (Hudgel 1994).

1.3.4. Bronchial hyperresponsiveness

Bronchial hyperresponsiveness (BHR) is the increased reactivity of the airways to a wide variety of pharmacological, chemical and physical agents (Kay et al. 1989, Casale 1988).

Responsiveness is usually measured by constructing dose–response curves to a stimulus (Cockroft et al. 1977). Asthmatic subjects, whether or not they show evidence

of specific hypersensitivity reactions, are abnormally sensitive to non-specific bronchoconstrictor agents. Among these, the chemical mediators histamine and methacholine (MCh) have been widely studied (Ryan et al. 1981, Woolcock et al. 1984, Xu et al. 1993). Responsiveness is often reported as the concentration or dose of inhaled agonist that causes a change in pulmonary resistance of a given magnitude or a fall in FEV_1 of 20% (PD_{20}). There is a considerable variability in the ability of the airways of different subjects to narrow in response to various stimuli such as MCh and histamine. These substances are frequently administered by aerosol in order to quantitate the ability of airways to narrow with provocation. Woolcock and coworkers (1984) and Sterk and associates (1985) found that normal subjects show a plateau on the dose-response curve to histamine and MCh. Ding et al. (1987) have confirmed that the dose-response curve to inhaled MCh in normal subjects reaches a plateau beyond which increasing concentrations of MCh do not elicit further increases in bronchoconstriction. Subjects with mild asthma have also been found to show a plateau, but the maximal response was increased (Woolcock et al. 1984). In subjects with moderate asthma, a plateau could not be demonstrated because large decreases in FEV_1 were obtained with submaximal doses of agonist.

The exact mechanisms underlying BHR are, however, still not known. It is likely that a variety of factors are involved including baseline airway geometry, autonomic nervous control of the smooth muscle, the smooth muscle cell itself, bronchial mucosal permeability, and epithelial damage and inflammation (Boushey et al. 1980, Casale 1988, Kay et al. 1989, Barnes 1985). Whatever the mechanisms of responsiveness, excessive airway smooth muscle shortening is likely to be a very important factor. Excessive narrowing could arise as a consequence of factors intrinsic to the smooth muscle itself such as changes in the amount of muscle (hypertrophy or hyperplasia) or as a result of loss of inhibitory factors limiting smooth muscle shortening. Elastic loads have the potential to act to limit shortening either through the non-deformability of cartilage or the mechanical interacters between the airways and the surrounding parenchyma (Morenoet

al. 1986). The structure of the airway wall may also be very important. Post-mortem asthmatic airway walls usually demonstrate thickening caused by edema and inflammatory cell infiltration (Hogg 1985). Increased airway wall thickness could contribute substantially to exaggerated airway narrowing (James et al. 1989).

Another potentially important factor is the geometrical arrangement of the smooth muscle on airway wall.

1.4. Models of ASM shortening

Wiggs et al. (1990) investigated the interaction between airway smooth muscle shortening and airway wall thickening on changes in pulmonary resistance in a human lung model of the tracheobronchial tree. The magnitude of narrowing during constriction was related to the degree of muscle shortening, the proportion of airway wall circumference occupied by muscle and the airway wall thickness. They also found an increase in resistance associated with decreased lung volume. A potentially important consideration in their study was the orientation of airway smooth muscle, which they assumed was circumferential for the sake of simplicity. The present work is an attempt to test this assumption.

In a theoretical analysis, Bates and Martin (1990) have demonstrated that, depending on the physical properties of the airway wall, airway smooth muscle structure and orientation could alter the way smooth muscle shortening is transduced into airway narrowing. In their study Bates and Martin investigated the following model: The airway was modeled as a cylinder of given wall thickness around which the muscle was wound as a spiral. The longitudinal and circumferential elasticities of the airway were embodied in a 2×2 matrix of elastic coefficients. They modelled smooth muscle shortening under three conditions: 1) a longitudinally stiff airway, 2) a circumferentially stiff airway, and 3) an airway that is both longitudinally and circumferentially compressible. If the airway

is longitudinally stiff and can only be compressed circumferentially, for a given degree of smooth muscle shortening, airway resistance will increase markedly with increasing pitch of the smooth muscle spiral. On the other hand, the muscle tension required to elicit a given change in resistance also will increase markedly with pitch (see figure 4 in Bates and Martin 1990). For the second condition, an airway that is circumferentially stiff, the effect of increasing pitch would be reversed. This condition however is unlikely to be present in real airways, since most airways are collapsible. When Bates and Martin modelled an airway that can be compressed both longitudinally and circumferentially, resistance first increased and then decreased as spiral pitch increased. Similarly, the muscle tension required to elicit a given change in resistance first increased and then decreased with pitch (see figure 8 in Bates and Martin 1990). Thus under most conditions airway smooth muscle orientation has potential to profoundly influence the way in which airway smooth muscle shortening is translated into airway narrowing.

1.5. Morphometric methods for the study of smooth muscle

1.5.1 Two-dimensional studies

The notion that airway smooth muscle fibres are arranged in a helical pattern relates to the observations of Miller (1937). He produced longitudinal sections of human airway wall which suggested to him that the airway smooth muscle was composed of a network of layers with helically arranged cell bundles. No quantitation of the orientation was done. Walmsley and colleagues (1982) using a microscope protractor and filar eyepiece to measure orientation of both arteriole smooth muscle and endothelial cell nuclei, found that smooth muscle orientation was not significantly different in dilated or contracted arterioles. The mean pitch angle was 1.1 ± 5.9° (N = 1000) with respect to the circumferential axis of the vessel.

1.5.2. Three dimensional reconstruction

Ebina and coworkers (1990a) used three-dimensional reconstruction to measure the angle of orientation of human airway smooth muscle in bronchi and found the average angle of orientation to be approximately 30°. They supplied no information, however, about the variation in angle of orientation of muscle fibres in their specimens either within the airway tree or between individuals.

1.5.3. Polarizing light microscope

Polarizing light microscopy has been used to measure spatial orientation of vascular smooth muscle by Finlay (1989). The principle of the method is based on geometrical relationships, and the smooth muscle cell can be measured in three dimension (3-D) orientation by vector or birefringence techniques. Finlay et al. established a method that requires a predetermined cutting angle for a segment of artery, therefore, this method is not well suited to sections of small airways.

The goals of my study were to determine if the findings of Ebina and coworkers (1990) could be generalized across species, and to determine the variability of airway smooth muscle fibre orientation across the airway tree. We chose to employ a method of en-face dissection. The technique involves sectioning the airway parallel to its long axis, an approach that has been used for descriptive purposes since the time of Miller (1937), but which has not been exploited for quantitation. We found this approach to be more efficient and simpler to use, especially for studies across many generations of the airway tree. We report the results of applying this method in four cats and one human.

2. METHODS

2.1. Materials and methods

2.1.1. Cat

The lungs were removed from 4 male adult cats (wt. 4.42 ± 0.54 kg). Specimens were fixed by intrabronchial infusion with 10% formalin at a constant pressure of 25 cmH_20 for 48 hrs at room temperature. The bronchial tree was dissected and removed from the left caudal lobe of each cat. The following procedures were used to prepare specimens for histological examination:

a) Dissection of bronchial tree After fixation, formalin was gently expressed from the lung and the airways reinflated with 2% coloured gelatin solution in order to distinguish between lung parenchyma and the bronchial tree. The trachea was clamped and the lungs were cooled to 4° C for 30 minutes to solidify the gelatin for easy dissection. Once cooled, the first bronchial branch (including the bronchi and bronchioles) from the left caudal lobe was dissected out carefully. The bronchial branch was dissected free of lung parenchyma tissue investments.

In the cat, relatively little information is available regarding the classification of airway generations, but it appears to have an analogous anatomic configuration to human and other large mammals (Donnersberger 1980, Yeh et al. 1979, West et al. 1986). We therefore used the method described by Weibel (1963) in order to classify airway generations, setting the trachea to be generation 0. Generation numbers then increased at each succeeding branch point.

b) Decalcification Airway generations 4 to 5, which have large cartilage plates, were immersed in Fisher Calex solution for 48 hrs.

c) Tissue dehydration The bronchial tree from generations 4 to 5 and from generations 6 to 8, were placed in separate tissue cassettes, and then processed through graded alcohols, xylene and paraffin overnight.

d) Dividing airway generations After dehydration processing, the bronchial tree was infused with paraffin, in order to harden the specimen and to minimize further

shrinkage. At this time, we could easily divide the bronchial tree into segments at branch points where each segment represents one generation. Airway generations 4 to 18 were cut transversely using a dissecting microscope.

e) Embedding, slicing and staining Segments of airways between branch points were embedded in melted paraffin blocks at 60° C in a longitudinal position. From each block, 5 μm thick serial longitudinal sections were cut parallel to the airway's long axis as shown in figure 1. Sections were obtained every 5 μm from the outer to the inner aspect of the airway wall. The tissue sections were mounted and stained with haematoxylin–phloxine–saffron (HPS). With this stain, the nuclei of smooth muscle cells were stained blue with a red cytoplasm, elastic fibres were stained yellow. Care was taken to ensure that the long axis of the airway could be identified. All sections from each generation were examined for airway smooth muscle content and the sections with a large quantity of muscle were used for measurement of smooth muscle orientation.

2.1.2. Human

One adult human left upper lobe was obtained from a surgical excision in a patient without bronchial asthma. The lobe was fixed in 10% formalin using the same conditions as above. Airway generations 4 to 22 were dissected and removed from the lingular division of the upper lobe. Airway generations 4 to 6 was cut off transversely and immersed in Fisher Calex solution for decalcification for 48 hrs. The bronchial tree from generations 7 to 22 was divided into two parts to accommodate the larger size of the airway tree. The remaining processing was carried out in a manner similar to that done with the cat airways.

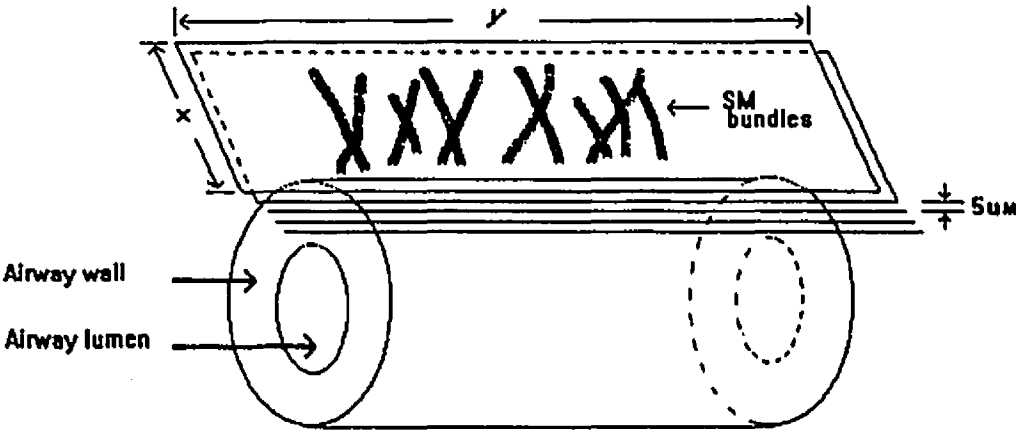

Figure 1. Schematic demonstrating the method of sectioning for preparation of specimens for measurement of smooth muscle orientation. Serial 5μm thick longitudinal sections were taken parallel to the long axis of the airway.

2.2. Morphometry

2.2.1. Establishing a measurement reference

A necessary part of studies of directional organization of tissue is the establishment of a reference against which measurements can be compared or evaluated. We attempted several methods, including the placement of markers in paraffin blocks and on slides, but found that the best reference was to use the anatomical organization of the airway wall itself. It has been known at least since Miller (1937) that elastic fibres run parallel to the long axis of the airway between branch points. Although the elastic fibres were generally parallel to the long axis of the airway, individual fibres swing up to 5°. This level of error is less than we obtained in preliminary studies of other techniques. It sets a lower limit on our ability to measure airways smooth muscle orientation.

2.2.2. Measurement of the angle of orientation

It has been previously observed that smooth muscle cells are spindle-shaped with a single centrally placed nucleus occupying the wide portion of the cell about midway along its length and elongated along the long axis of the fibre (Leeson 1976). Smooth muscle cells are rarely multinucleated and nuclei have been previously used for verification of the presence of hyperplasia in the airways (Fiore 1989). As the nuclei are more easily seen than the cells themselves, but are oriented parallel to axis of the cells, they are suitable for measurement of the orientation of airway smooth muscle fibres.

We attempted to measure 100 nuclei per section. We measured nuclear orientation by following the vertical line of the cross-hair from top to bottom. Every nucleus touching this vertical line was measured. If we could not find 100 nuclei in one slide, the next serial section of the same airway generation was studied, until all sections for that generation had been studied.

All measurements were carried out using a conventional light microscope (Leitz, New Jersey) at 250X magnification. The microscope was equipped with a cross-hair in the eyepiece which was used as a marker to define the orientation of the airway. The

slide was placed on a rotating microscope stage, and the cross-hair was aligned with the longitudinal axis of the tissue section. The microscope was equipped with a drawing tube attachment, which was used to observe the tracer from the digitizing tablet (Jandel Scientific, Corte Madera, CA), which was superimposed on the microscope image (Figure 2). A computer software package (Sigma-Scan, Jandel Scientific, Corte Madera, CA) was used to measure the angles from the projected images. The angle of orientation was taken as arc tan y/x where y was the projection of a cell nucleus along the longitudinal axis and x its perpendicular (Figure 3).

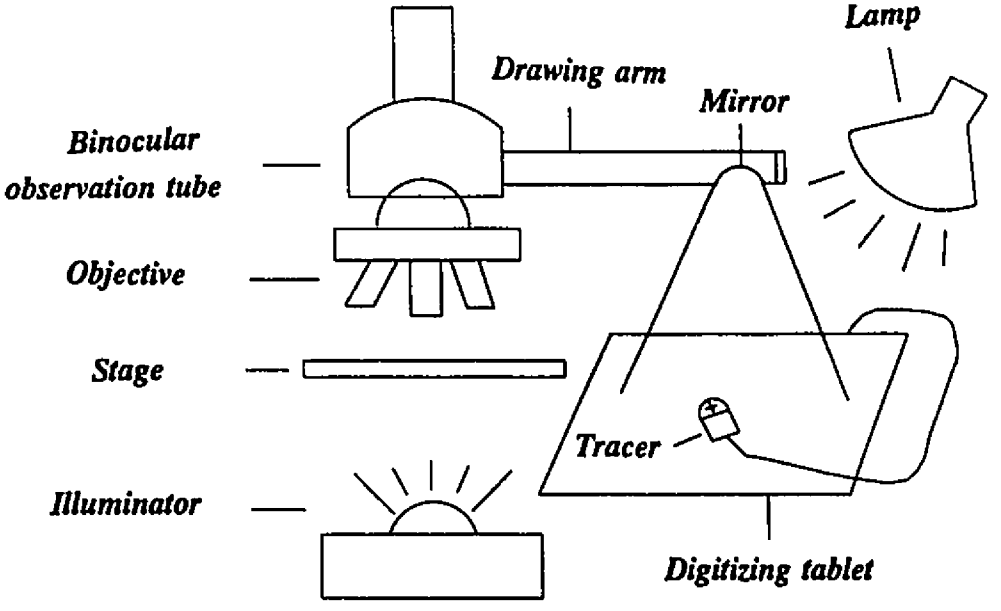

Figure 2. Schematic presentation showing the measurements for airway smooth muscle orientation of the equipment setting.

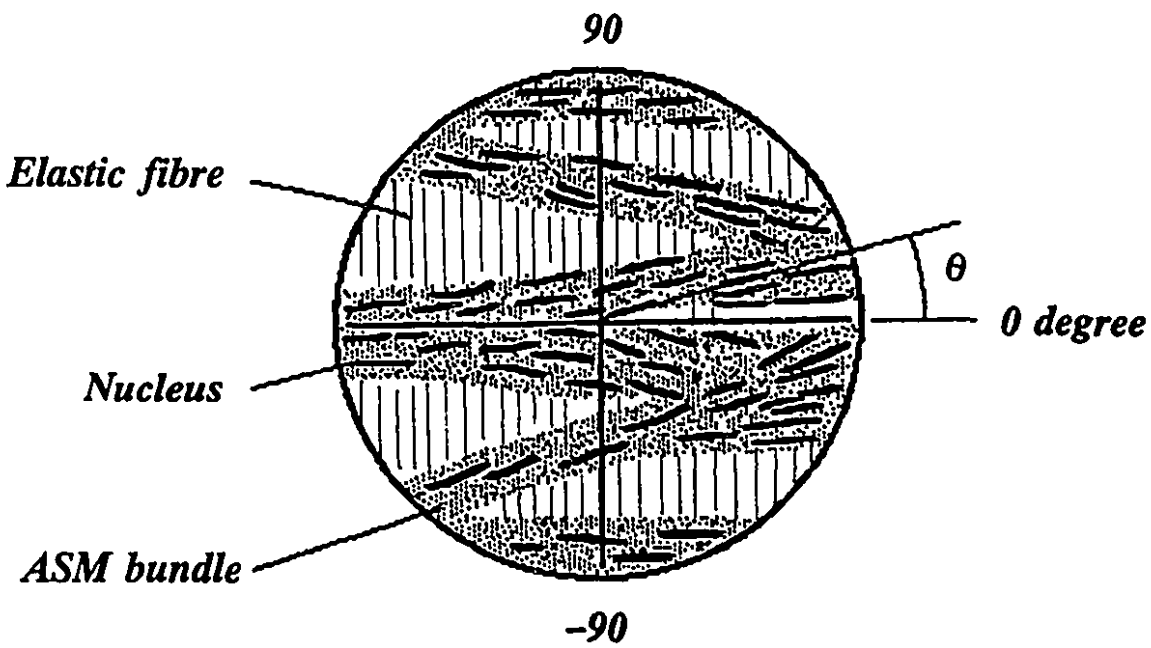

Figure 3. Schematic demonstrating the method of angle measurement for airway smooth muscle cell nuclei. Angles were measured from centre of the light microscopic field, and angles are expressed as values from –90° (clockwise) to 90° (counterclockwise).

2.3. Data analysis

For the purpose of obtaining precise nuclear angles, sampling was done with the goal of measuring up to 100 nuclei per airway generation from several serial sections. When the slide with the dissected airway was positioned in the microscope for angle measurements, we made sure that the side corresponding to the higher generation, ie the periphery of the lung was positioned away from the observer. Angles were measured as positive or negative in the standard counter clockwise way with respect to a line transversal to the axis of the airway. This means that a nucleus with a positive angle was positioned on a right handed spiral towards the peripheral airways. Conversely, a nuclei with a negative angle was positioned in a left handed spiral.

Since only one line was utilized to sample nuclei in each airway, when repetitions of the measurements were performed, a different set of nuclei was used. In order to verify the reproducibility of our measurements, we carried out a correlation between two readings of airway smooth muscle angles by different individuals. We plotted the measurements of two independent observers as shown in Figure 4. We denoted the sorted data values for the angle of nuclei from observer 1 as $y_{(1)}$ to $y_{(100)}$, and the sorted data values for the angle of nuclei from observer 2 as $x_{(1)}$ to $x_{(100)}$. This method is know as a 'Quantile–Quantile Plot' (Q–Q Plot) (Chambers et al. 1983). Reproducibility within observers was measured using linear regression.

The Q–Q Plot is used to compare two distributions. If we have 2 samples and we want to verify graphically the hypothesis that the distributions are similar, we independently order both samples from small to large values. With two samples of the same size, as in our case, we simply plot the corresponding ordered values against each other. If the distribution of both samples are similar, the points will fall over the identity line. If the first sample has more spread, then we will obtain a straight line with a smaller slope than the identity line; if the first sample is more spread only in the tails, then we obtain an S type of curvature in the line. A simple shift of the identity line upwards will indicate that the first sample is uniformly larger than the second sample.

We produced Q–Q Plots from some of the slides about the angle measurements between observers, and found the interobserver correlation was high when angles were calculated as angles between 0° and 90° by using this method (r=.987). The most reproducible part within observers was found at angle between 5° to 20°. The relatively poorer correlation was at angles less than 5°. This may be because the small angles were difficult to measure accurately.

We also made a comparison of angle measurement variability within observers for the two readers. Our results demonstrate the intraobserver correlation reproducibility was high: the correlation of coefficients were 0.94 for observer 1, and 0.97 for observer 2.

All angles were expressed by the means and their standard deviations.

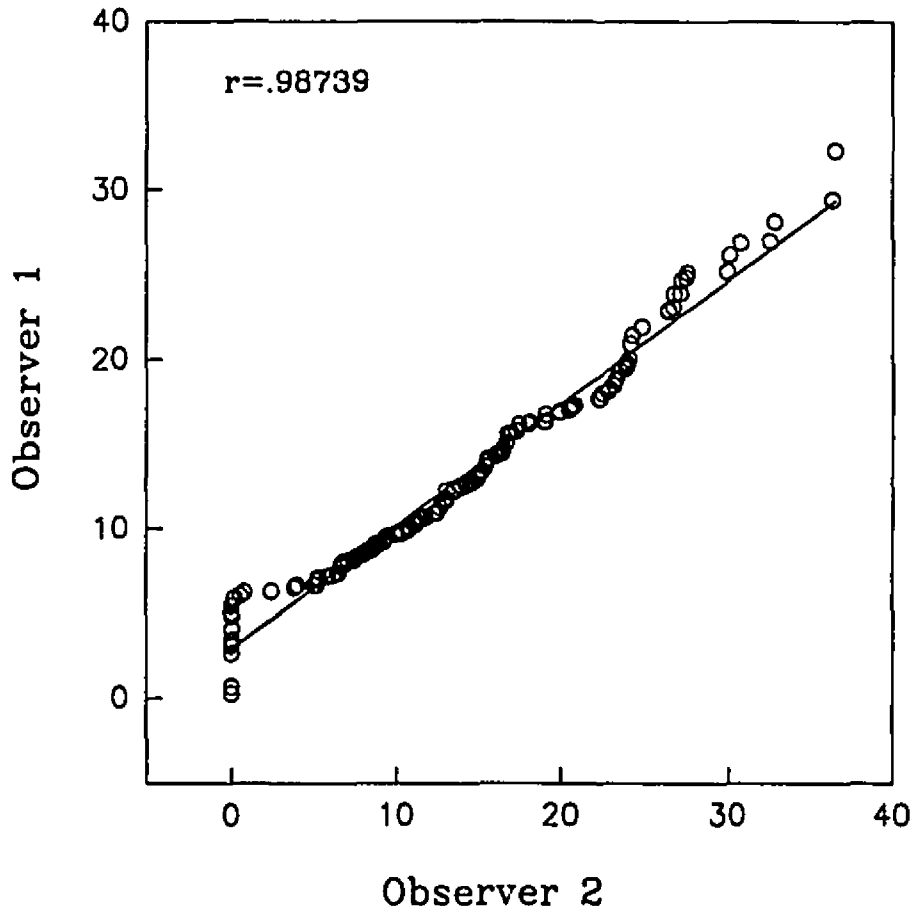

Figure 4. Reproducibility between observer 1 and observer 2 was compared by a Q-Q plot. A high correlation was found with r=.987.

3. RESULTS

3.1. Light microscopic observation

We were interested in observing the structure of airway smooth muscle, including its arrangement along the airway wall. Figure 5 shows a photomicrograph of airway smooth muscle cut in longitudinal section at 100X magnification; the principal axis of the bronchus runs vertically. Each panel represents one individual airway generation. Smooth muscle fibres were elongated with a cigar-shaped nucleus. They lie approximately parallel to each other, and fibres were organized into bundles largely separated from one another by spaces filled with connective tissue. These muscle bundles run nearly transversely with their characteristic criss-cross pattern around the airway wall. There was a tendency for smooth muscle bundles to become more sparse this in the smaller airways.

The numerous elastic fibres stained yellow were easily seen and ran discontinuously between smooth muscle sheets on the same histological sections. Although the elastic fibres were not absolutely straight, in general they followed a longitudinal course. Some of them are slightly wavy, however we found that the maximum variation was less than 5°.

The mucous glands lie on the sides and beneath the smooth muscle layer, and numerous glandular ducts pass between the muscle bundles. In these sections, the cartilage plate and connective tissue are also shown clearly.

Figure 5. A (generation 5) & B (generation 8)

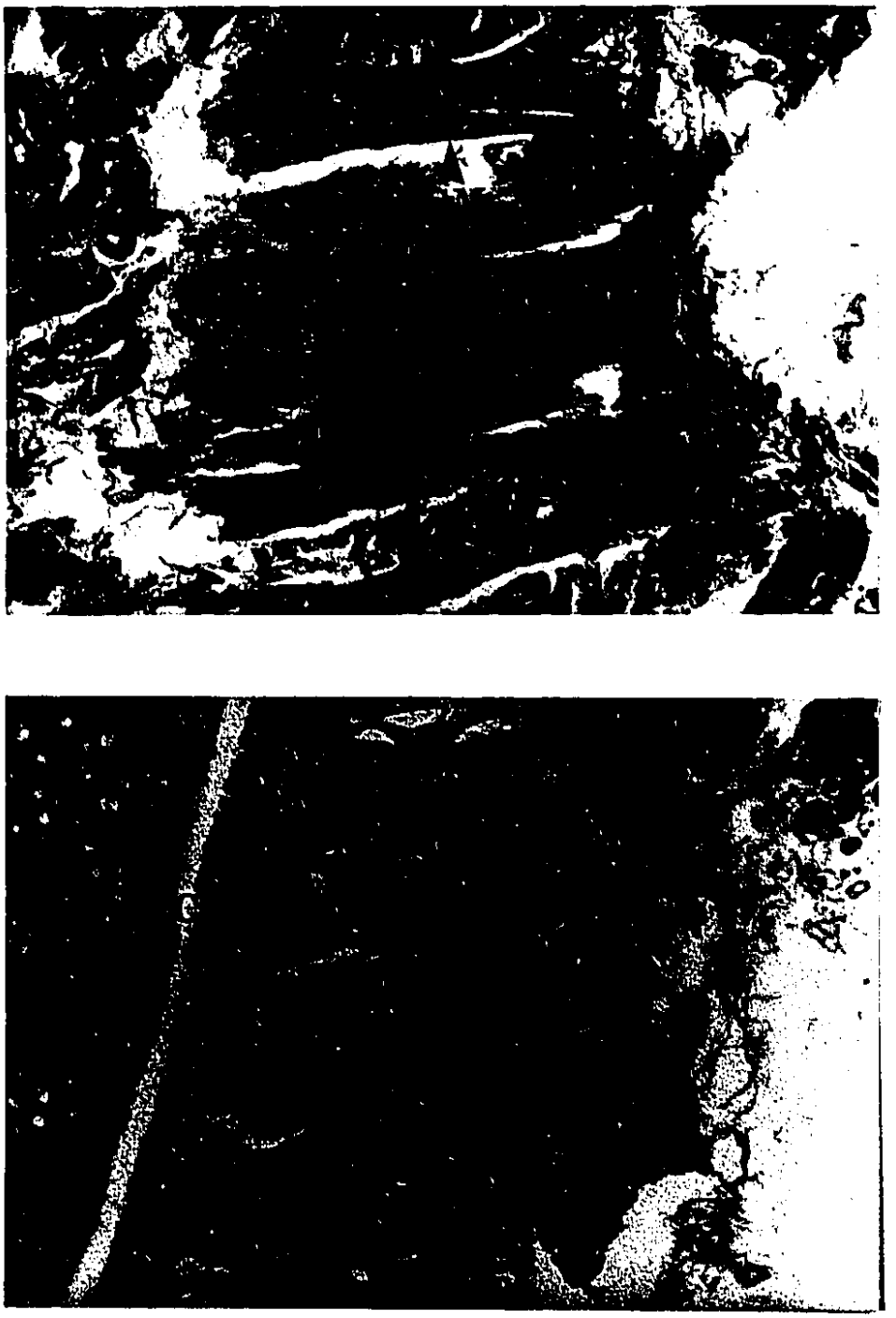

Figure 5. C (generation 12) & D (generation 16)

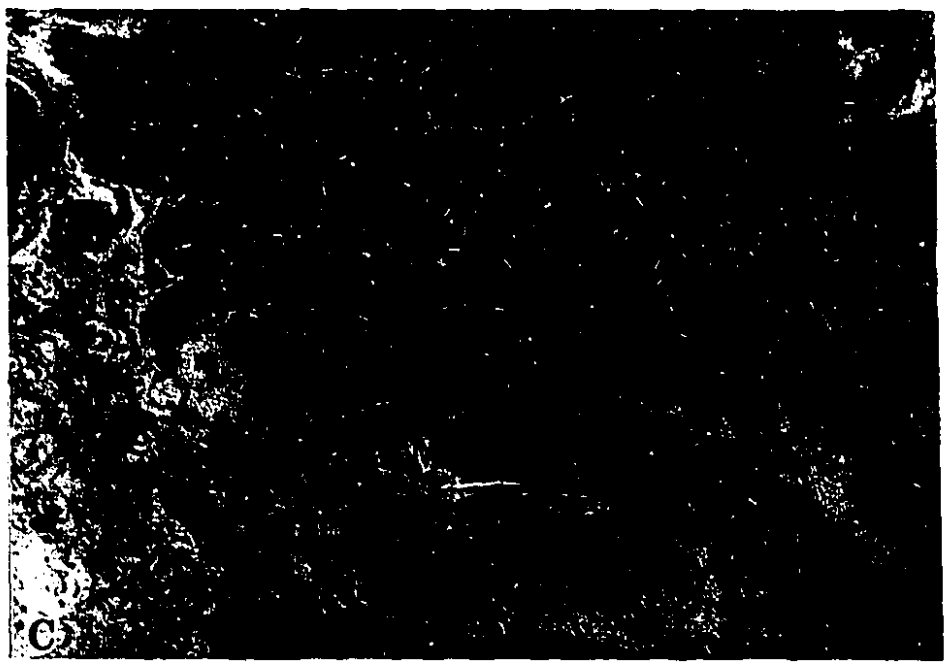

Figure 5. Photomicrograph of longitudinal sections with airway smooth muscle bundles (SM) in nearly transverse direction, and with longitudinal direction of elastic fibres (EF) from generation 5 (A), 8 (B), 12 (C) and 16 (D) at magnification (100X). Labelled C is cartilage.

3.2. Morphometric findings

Table 1 shows the average numbers of airway smooth muscle nuclei measured per generation of each cat. The average number of nuclei measured was similar among cats, ranging from 65 to 79. On the other hand, there was a large difference in the numbers of nuclei in individual generations from larger to smaller generations (range: 102 to 29). This variation was similar among the 4 cats; all cats had the same variance of nuclei numbers (Table 1).

Table 1

The Number of Nuclei Counted Per Generation Per Animal

Subject	Mean	SD	Range
Cat #1	69.1	23.9	29–102
Cat #2	79.2	21.1	57–101
Cat #3	65.5	24.5	51–102
Cat #4	75.0	29.8	32–96

The average numbers of smooth muscle cell nuclei per generation in 4 cats. The small quantity of nuclei are found in distal bronchioles.

3.3. Shrinkage measurement

The fixation process is associated with shrinkage. In order to determine the magnitude of the shrinkage we made two measurements of airway smooth muscle before and after fixation in specimens of both trachea and lung parenchyma. Because they have different histological structure and components, the shrinkage in two regions may not be the same. Changes in dimensions are defined by the shrinkage factor (f) (Eq. 1), and the effect of shrinkage on measurements of airway smooth muscle orientation as follows:

(1) eg. The shrinkage factor for the trachea length and width

$f_L = 1-(L-L')/L$

$= 1-(1.1-1.05)/1.1 = 0.955$

$f_W = 1-(W-W')/W$

$= 1-(0.95-0.85)/0.95 = 0.895$

(2) The angle of orientation of the smooth muscle (θ) equals arctan L/W

$\tan \theta$ meas = $L/W = y.f(y)/x.f(x)$

$= (y/x).(f(y)/f(x))$

$= f(y)/f(x)$

$\tan \theta = L/W = 0.955/0.895$

$= 1.067$

(3) $\tan \theta' = \tan \theta / \tan \theta$ meas

eg. assume a true angle of 10°

arctan L/W=10°

for shrinkage $L' = L \times f_L$

$W' = W \times f_W$

Measured angle after shrinkage

$\tan \theta$ L/W = arctan L'/W'

$\tan \theta / \tan \theta$ meas = $\tan \theta'$

The angle could be 9.36°

* L = before length of tissue (cm)
* L'= after length of tissue (cm)
* W = before width of tissue (cm)
* W'= after width of tissue (cm)
* f = factor
* y = tissue long axis
* x = tissue transverse axis
* tan θ'= shrunken tangent

Table 2 shows the dimensions of the lung parenchyma and trachea before and after fixation. Tissue length and width were used to calculate the shrinkage factor. We found that the shrinkage factor varied between trachea and lung parenchyma from 0.9 to 0.8, indicating that lung parenchyma shrank more than trachea. The volumetric shrinkage was estimated at 14.6% in trachea and 34% in lung parenchyma. These results are similar to that of Weibel (1968). Although shrinkage has an important effect on estimates of volume it has a much smaller effect on measurements of angle. This is because the tissue shrinks in a reasonably isotropic manner.

With respect to the angles, we found the difference was less than 10% (Table 3). We have therefore made no corrections for shrinkage in our results.

Table 2

Tissue Shrinkage After Fixation

		Tissue fixation		Shrinkage factor
		Before	After	
Trachea	Length	1.1	1.05	0.955
	Width	0.95	0.85	0.895
Lung parenchyma	Length	2.15	1.80	0.837
	Width	1.05	0.82	0.781

Tissue length and width expressed by a unit of centimetre.

Table 3

The Relationship Between Tissue Shrinkage and ASM Angle Changes

	Measured Angle (degrees)	Corrected for shrinkage Angle (degrees)
Trachea	10	9.37
	20	18.84
	30	28.40
Intrapulmonary airway	10	9.32
	20	18.78
	30	28.29

3.4. Distribution of orientation of ASM

When we analyzed the orientation of airway smooth muscle nuclei, it was found to exhibit both negative and positive angles. Figure 6 shows the distribution of orientation of the airway smooth muscle nuclei across the airway tree in cat 1. One can see that most of the angles lie between -20° and 20°. Although smooth muscle orientation varies across generations, there was a clustering of fibre angle between -40° and 40° in all generations.

In Figure 7, two dimensional plots of angles from the 4 cats for generations 4, 8, 12 and 16 demonstrate that there is a similar distribution of orientation in smooth muscle between animals at any given generation. A remarkable feature was the presence of asymmetrical peaks in the distribution among all generations. There was a tendency to favour clockwise winding especially in the larger generations.

Figure 8 shows the distribution of orientation of the airway smooth muscle fibres in each individual subject. There was a tendency for the higher generation airways to have a larger proportion of muscle fibres with a negative angle of orientation. Positive angle fibres have a small tail of distribution. All subjects showed an asymmetrical orientation.

When the airway generations were divided into four groups for cat 1, the distribution varied among them (Fig. 12). In large airways, the distributions were narrower than in medium and small airways; a flat distribution was found in peripheral airways. There was a large variance in the angles in small generations.

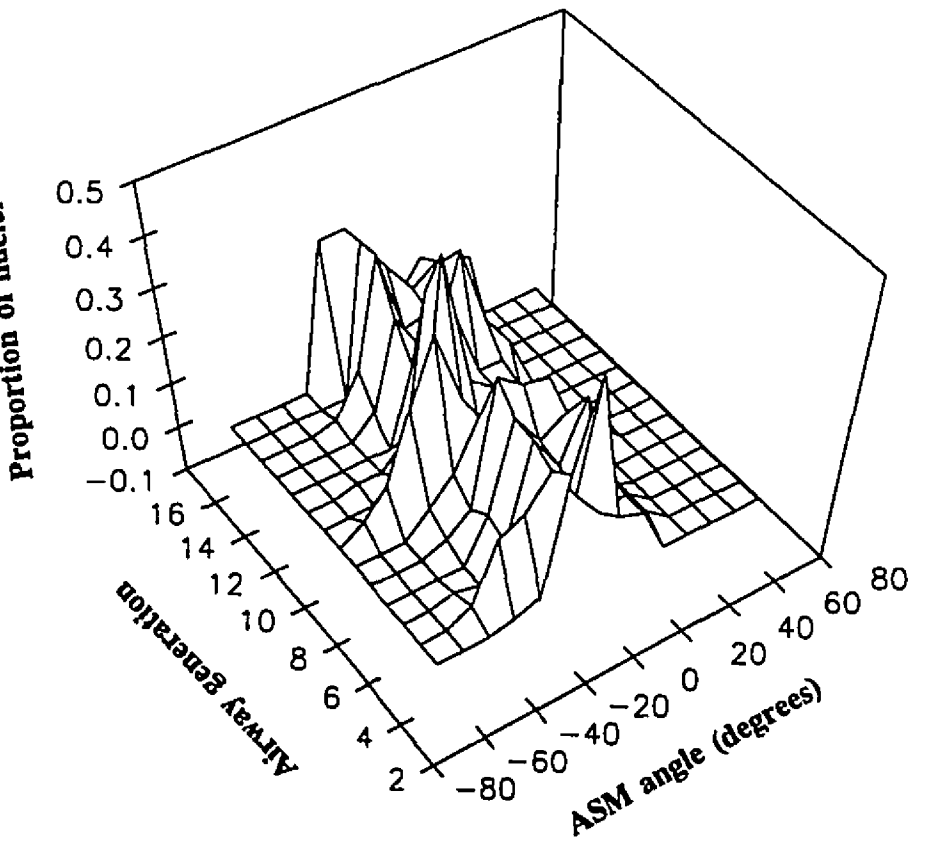

Figure 6. The distribution of orientation of airway smooth muscle cell nuclei in systematical generations through the airway tree. Proportion of nuclei on Z–axis against airway generations 4–17 on x–axis and airway smooth muscle angle (degrees) on y–axis for cat 1. Most nuclei lay between −20° to 20° in all generations.

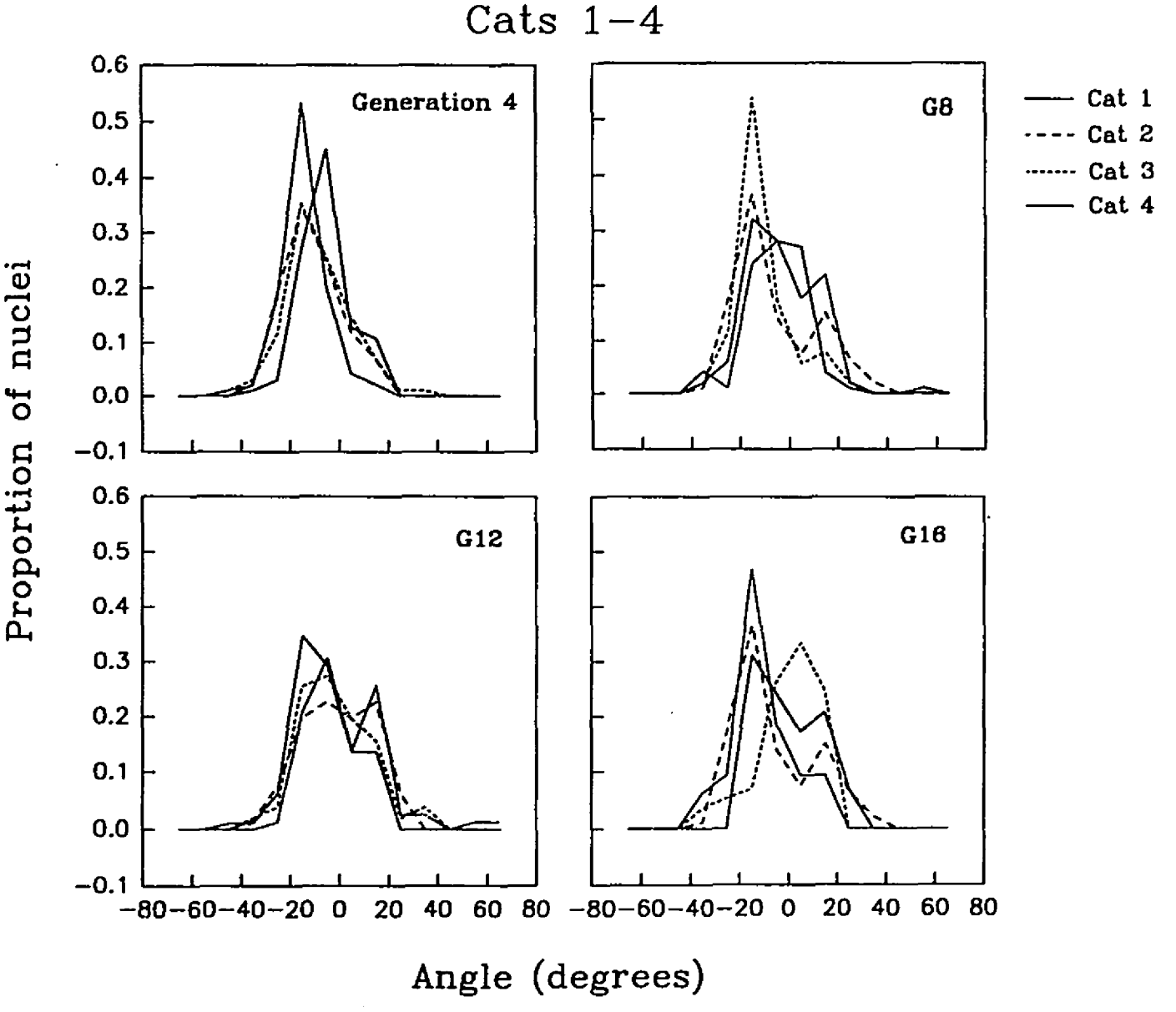
Cats 1–4
Generation 4
G8
G12
G16
Cat 1
Cat 2
Cat 3
Cat 4
Proportion of nuclei
0.6
0.5
0.4
0.3
0.2
0.1
0.0
−0.1
−80 −60 −40 −20 0 20 40 60 80
Angle (degrees)

Figure 7. Proportion of nuclei of each generation plotted against angles of nuclei in degrees. Each line represents per generation per cat. Between four animals, the angles of distribution were very similar in equivalent generations.

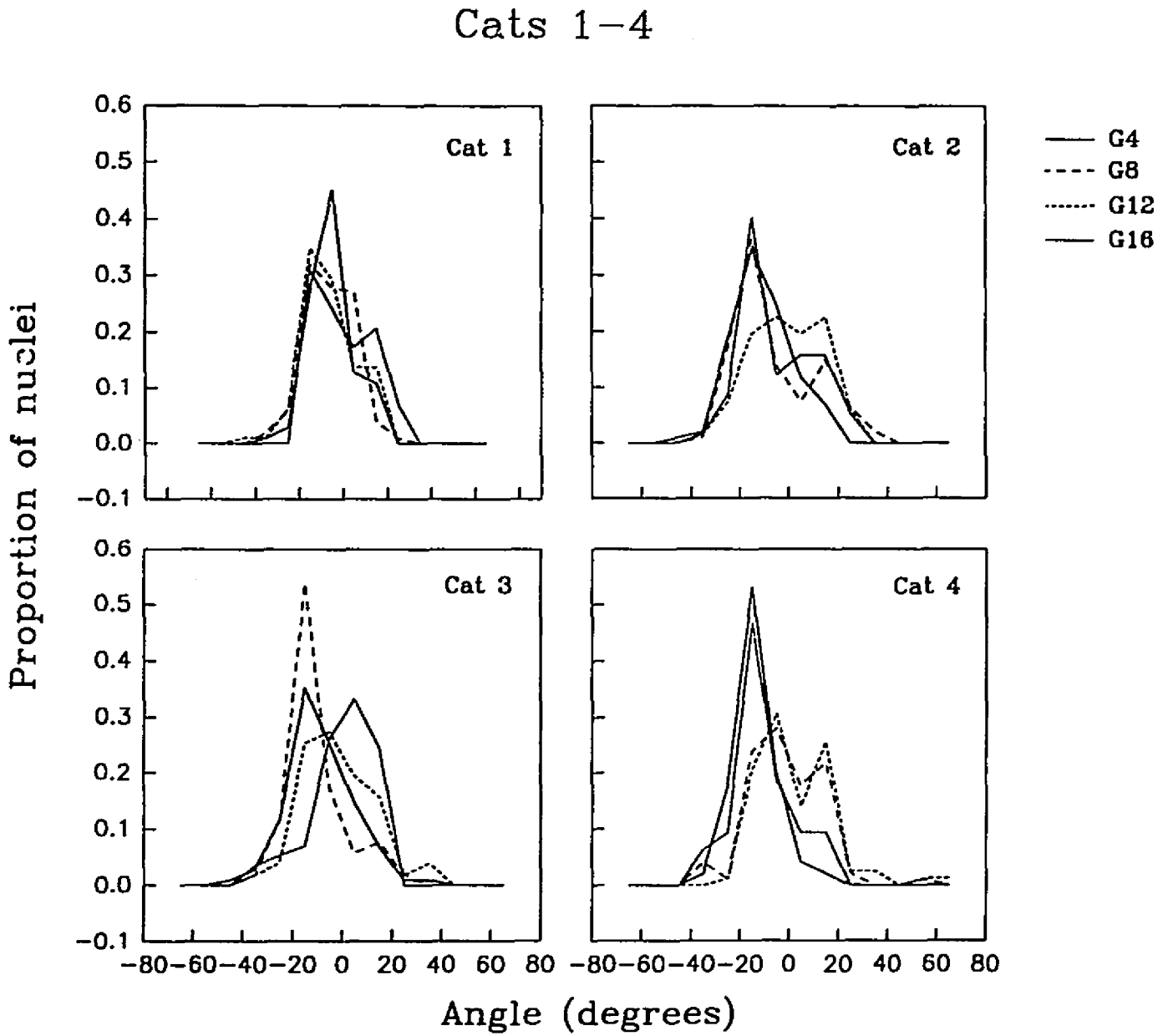
Cats 1–4
Cat 1
Cat 2
Cat 3
Cat 4
G4
G8
G12
G16
Proportion of nuclei
0.6
0.5
0.4
0.3
0.2
0.1
0.0
−0.1
−80 −60 −40 −20 0 20 40 60 80
Angle (degrees)

Figure 8. Angle distribution in four generations in each cat plotted as individual figures. The results of four cats for airway generations 4, 8, 12, and 16 found the angle tends to be clockwise.

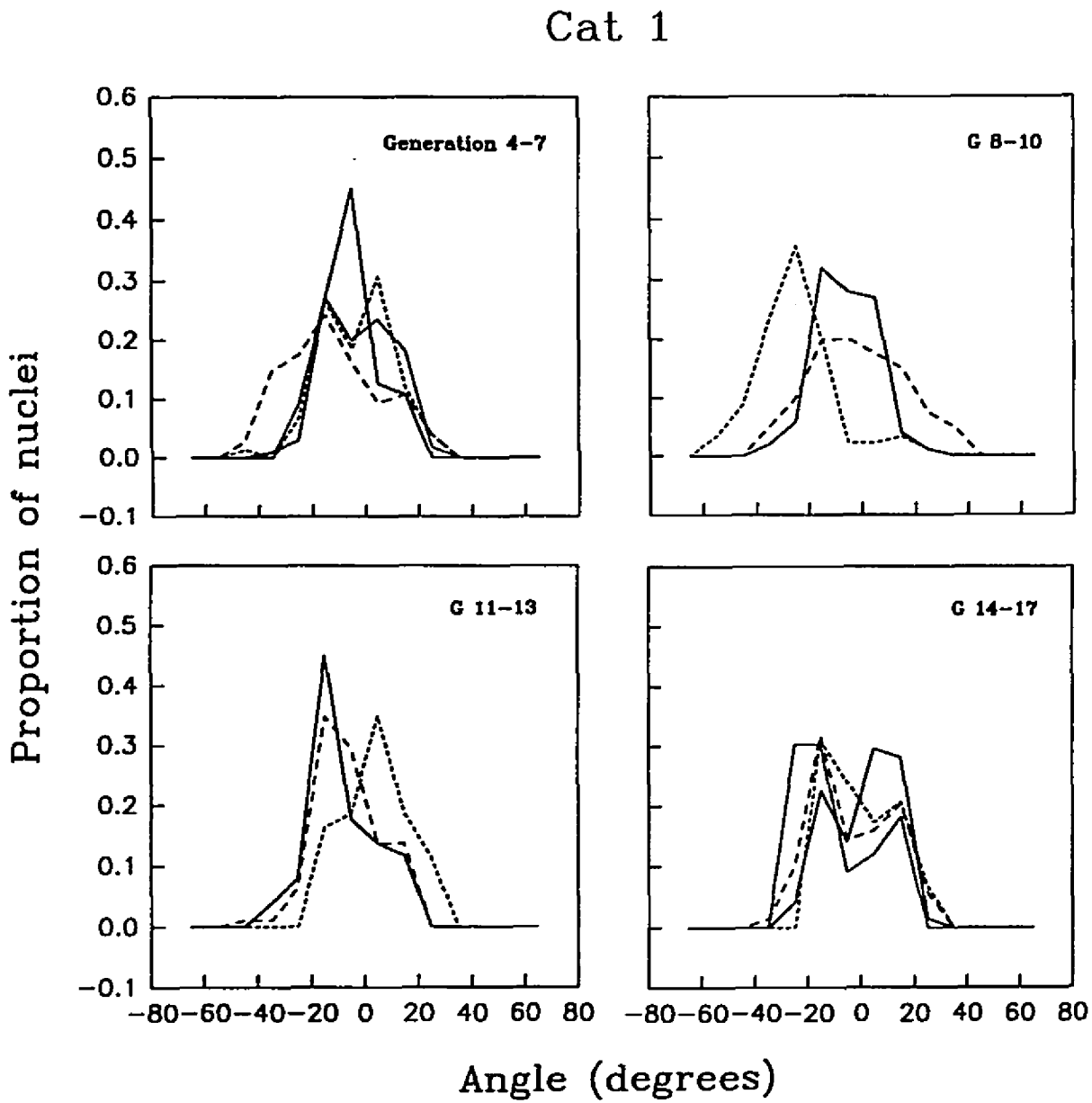
Cat 1
Generation 4-7
G 8-10
G 11-13
G 14-17
Proportion of nuclei
0.6
0.5
0.4
0.3
0.2
0.1
0.0
-0.1
-80 -60 -40 -20 0 20 40 60 80
Angle (degrees)

Figure 9. Airway generations separated into four groups for cat 1. There are narrower distributions in large airways, and flat distributions in peripheral airways.

Results

Table 4 shows the mean angles and standard deviation of orientation of the airway smooth muscle for four cats. There were very similar angles found from 12 to 14° in 4 cats in multiple airway generations when the angle was counted as a value between 0–90° (acute angle). Standard deviations were small except in cat 1. The overall mean angle was 13.2°.

Table 5 shows the mean angles across generations in cat 1. A few generations have large mean angles, but most have very similar values, especially in small generations where angles were relatively constant.

Although there was some variation in the mean angles across airway generations of cat 1, findings were similar in the other three cats (Table 6).

Table 4

The Angle of the ASM Nuclei in Each Subject

Subject	Mean angles	SD
Cat #1	13.5	4.5
Cat #2	13.9	1.8
Cat #3	12.3	1.6
Cat #4	13.2	1.3
Overall mean	13.2	

Airway smooth muscle angle expressed as the value between 0–90°. The mean angle was very consistent among animals and across generations.

Table 5

The Mean Angle in Systematic Airway Generation in Cat #1

Generation	4	5	6	7	8	9	10	11	12	13	14	15	16	17
Mean	9.8	18.4	10.8	11.7	10.6	15.2	26.8	12.7	11.4	10.8	10.6	14.4	10.8	14.9
SD	5.6	10.4	7.3	5.3	6.8	8.9	11.2	6.8	6.7	6.7	5.1	6.5	5.0	7.0

Angle in individual generation was different at center airway, constant angle was found in small airway. Mean angle in cat 1 was 13.5.

Table 6

The Mean Angle, median and Percentile in Cats

Generation	4			8			12			16		
Cat number	2	3	4	2	3	4	2	3	4	2	3	4
Mean	14.2	13.3	14.2	15.5	13.7	11.5	12.0	12.0	13.0	13.9	10.1	14.2
Median	11.5	11.6	13.3	14.8	12.8	10.3	11.1	10.1	10.8	13.5	8.4	12.3
75%	17.2	17.9	17.0	20.1	16.6	14.5	15.3	16.1	15.1	14.7	13.0	16.5

Figure 10 shows human airway smooth muscle orientation from generation 5 to 22. It has a very similar plot to the cats. Most of the angles lie between −20° and 20°, the only difference was the human data tends to be counter clockwise. Although smooth muscle orientation varies from maximal angle 16.6° to minimal angle 9.2° across generations, we found the average angle in human airways was 12.9° ± 2.2 when the angle was calculated as the value between 0–90°, very close to the value in the cat.

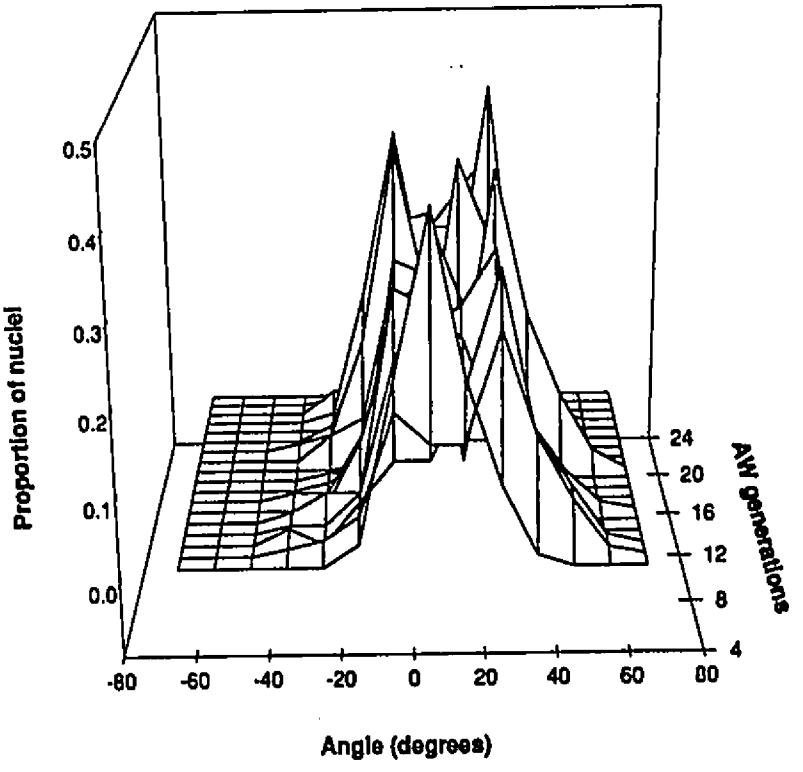

Figure 10. Human airway smooth muscle orientation distribution through generation 5–22. It has similar angles to the cat.

4. DISCUSSION

4.1. The measurement technique

This is the first report of a systematic study of the orientation of airway smooth muscle fibres across the airway tree. We used a method based on two dimensional (2–D) histological sections cut along the longitudinal axis of the bronchial wall (en–face dissection). Our results indicate that en–face dissection is a direct, reproducible method of measuring airway smooth muscle orientation across many generations of intraparenchymal airways. Although we found variation in orientation within airways, the mean angle of airway smooth muscle was consistently between 10° and 15° with reference to the transverse axis of the airway.

4.2. Sources of Error

A major potential source of error in measurements of fixed pulmonary tissue is the influence of shrinkage after fixation. According to Thurlbeck (1967) the major portion of tissue shrinkage results from dehydration. The maximum error that could be introduced in our measurement of airway smooth muscle orientation can be calculated from shrinkage data. To estimate shrinkage, we compared fixed tissue to processed tissue in two dimensions by measuring the length and width of fixed tissue as compared to unprocessed tissue (Table 2). From these data we estimated the effect of shrinkage on measurements of nuclear angle. Our results demonstrate that both tracheal and parenchymal shrinkage led to a decrease of less than 2° in the angle of airway smooth muscle (Table 3). As this error was small relative to the mean angle of 13°, we did not correct for shrinkage in our measurements.

4.3. Reproducibility

We found the technique to be adequately reproducible both within and between observers, except for measurements of nuclei oriented nearly circumferentially where more variability was seen. This suggests that we cannot exclude the possibility that the true angle is somewhat less than we measured.

4.4. A comparison between 2-D and 3-D

It is of interest to compare our results to those reported by Ebina and colleagues (1990_a). Using three dimensional reconstruction, they set out to quantify airway smooth muscle in peripheral airways (1993) as well as to look for evidence of hyperplasia and hypertrophy in asthmatic and COPD airways (1990_b). In the course of these studies they noted that airway smooth muscle was orientated obliquely and stated that the average angle of orientation was about 30°. This result is considerably higher than our own. It is hard to judge the adequacy of their measurements as no information was given regarding the exact technique used to measure orientation, nor do they report any systematic study across airway generations. Finally no information is given in their paper about the amount of variability they encountered.

We decided not to use three dimensional reconstruction to make our measurements. In a preliminary experiment we did carry out a reconstruction of a single airway segment. This required the preparation and measurement of over 100 two dimensional 5 μm thick cross-sections for a single generation. The final result, while similar in quality to that shown by Ebina et al. (1990_a) in their paper, was not suitable for accurate measurement of smooth muscle orientation. This is because it is difficult to distinguish

individual muscle layers. We found the technique to be far too cumbersome for use in measuring orientation across many airway generations.

4.5. The distribution of the ASM

The smooth muscle fibre orientation within the larger airways has been previously described (Miller 1937). Tracheal smooth muscle appears to have two layers: most fibres are arranged in the main bundles perpendicular to the airway axis; a smaller number of fibres run longitudinally along the airway. He reported that within the lobar and segmental bronchi there is a transition to a more helical orientation, although there is not much deviation from the circumferential. Our findings indicate that, in the cat at least, the smooth muscle of the intraparenchymal airways is on average oriented at a slight angle to the circumferential.

It is somewhat simplistic to discuss the angle of orientation as a single number since our data demonstrate considerable variation in angle within each generation. The angle varies between $-40°$ and $40°$ with the bulk of the angles between $-20°$ and $10°$. The distribution is asymmetric, particularly in the more proximal airways. Airway smooth muscle orientation clearly favours one direction of coiling over the other. Although this finding is intriguing, there is no obvious explanation for it. Smooth muscle has been described as being helically arranged in other tubular structures including the gut (McKirdy and Macmillian 1971 and Elsen and Arey 1966), the ureter (Matsuno et al. 1984), and the vasculature (Kockx et al. 1993). In those organs, the musclaris is far more complete than in the airways and muscle fibres are arranged in well defined layers which may run perpendicular to each other. The airway smooth muscle serves both as a connective tissue support as well as permitting propulsion in most of these tissues. In contrast, in most species the airways have relatively little muscle and appear to depend

on cartilage, other connective tissue, and the surrounding structures for mechanical support, particularly in the large airways.

4.6. ASM orientation and airway narrowing

Airway smooth muscle orientation has the potential to influence the mechanics of airway narrowing by influencing the vector of forces acting on the airway wall during bronchoconstriction. The theoretical basis for this has been discussed by Bates and Martin (1990). Briefly, depending on the mechanical properties of the airway wall, a portion of the force developed during airway smooth muscle shortening could act to shorten the length of the airway as well as to lead to airway narrowing. The greater the angle of orientation, the more likely for some change in airway length to occur. Current approaches to the modelling of airway narrowing assume that smooth muscle fibres are arranged circumferentially (Wiggs et al. 1991, 1992). To the extent that this assumption is true, it is assumed that all of the mechanical effects of airway smooth muscle shortening are translated into circumferential narrowing. If the true angle of orientation differs significantly from this, then predictions of the narrowing of the airway during bronchoconstriction will overestimate the degree of bronchoconstriction.

Although we observed that airway smooth muscle was not circumferentially oriented, we found only a small deviation from this in most airways studied. Furthermore, although airway smooth muscle orientation systematically favoured clockwise winding over counter-clockwise winding, all airways had significant fractions of the airway smooth muscle in both orientations. Based on these findings, we would not predict much change in airway length during bronchoconstriction unless the properties of the airway tree were such that the longitudinal rigidity of the airways was far less than its circumferential rigidity.

In support of this conclusion it is worthwhile to reexamine the airway model made by Bates and Martin (1990). In their theoretical model, they considered different conditions for the airway shortening. If the airway is longitudinally stiff, airway length remains constant. On the other hand, lumen radius and muscle tension, change with muscle shortening, and both are highly sensitive to muscle orientation. For example, when θ is between 0° to 15° the muscle is able to shorten around 40% of its original length before the lumen disappears, whereas when θ is 30° complete airway closure occurs before the muscle has shortened by less 30%. Similarly, the muscle tension increases at a rate orders of magnitude greater when θ is 30° than when it is between 0° to 15°. If an airway is able to change in both X and Y dimensions, in contrast to the previous, the effect of θ on the quantities shown is not monotonic. For example, for a given degree of muscle shortening, lumen radius first decreases with increasing θ and then begins to increase again. Nevertheless, when θ is 0° the muscle shortens by 40% of its original length without airway closure, whereas when θ is 15° airway closure occurs just as the muscle has shortened by 40%. When θ is 30° complete airway closure occurs before the muscle has shortened by even 30%. The muscle tension increased in angles at 30° is more than in angles at 15°.

Our average angle of orientation of airway smooth muscle is remarkably similar to that reported recently by Opazo-Saez and her colleagues (1994 abstract), who measured the longitudinal isometric tension and circumferential isometric tension for the isolated rabbit intraparenchymal airway smooth muscle, and inferred its orientation to be approximately 12°. That such a similar result was obtained with an independent technique in another species provides strong support for our results.

4.7. Conclusion

We measured airway smooth muscle orientation by measuring the angle of orientation of airway smooth muscle nuclei in airways sectioned parallel to their long axis. Although we observed considerable variation in angle of orientation in each generation, these distributions were consistent across generations and between individuals. Our findings suggest that airway smooth muscle fibre orientation differs only slightly from circumferential in normal airways, suggesting that the orientation of airway smooth muscle may not be a major factor in bronchoconstriction. Nevertheless, it is important that fibre orientation be taken into account in modelling studies of bronchoconstriction. Furthermore, it is unknown to what extent our findings are applicable to described airways where remodelling has the potential to alter both airway smooth muscle geometry and airway wall mechanical properties.

5. BIBLIOGRAPHY

American Thoracic Society (1962): Chronic Bronchitis, Asthma, and Pulmonary Emphysema. A statement by the committee on diagnostic standards for nontuberculous respiratory diseases. Am Rew Respir Dis 85: 762–768

Amiri MH and Gabella G (1988) Structure of the guinea-pig trachea at rest and in contraction. Anatomy and Embryology. 178(5): 389–97

Barnes PJ (1985) Adrenergic and non-adrenergic mechanisms in asthma. Prog Respir Res 19: 159–164

Barnes PJ (1987) Airway neuropeptides and asthma. Trends pharmac Sci 8: 24–27

Barnes PJ (1988) Inflammatory mediators and asthma. Pharmacological Reviews. 40(1): 49–84

Barnes PJ (1989) New concepts in the pathogenesis of bronchial hyperresponsiveness and asthma. J Allergy Clin Immunol 83: 1013–1026

Barnett K, Jacoby DB, Lazarus SC and Nadel JA (1987) Bradykinin stimulates release of an epithelial cell product that inhibits smooth muscle contraction. Am Rev Respir Dis 135: A274

Bates JHT and Martin JG (1990) A theoretical study of the effect of airway smooth muscle orientation on bronchoconstriction. J Appl Physiol 69(3): 995–1001

Bloom W and Fawcett DW (1975) A textbook of histology. 10th ed. Saunders, Philadelphia. Pp 288–290

Boushey HA and Holtzman MJ, Sheller JR and Nadel JA (1980) State of the art. Bronchial hyperreactivity. Am Rev Respir Dis 121: 389–413

Brewster CEP, Howarth PH, Djukanovic R, Wilson J, Holgate ST and Roche WR (1990) Myofibroblasts and subepithelial fibrosis in bronchial asthma. Am J Respir Cell Mol Biol Vol. 3. Pp 507–511

Chambers JM, Cleveland WS, Kleiner B and Tukey PA (1983) Graphical methods for data analysis. Wadsworth international. Pp 48–57

Chiasson RB & Booth ES (1982) Laboratory anatomy of the cat. Wm. C. Brown Company Publishers. Dubuque, Lowa. Pp 70–71

Casale TB (1988) Bronchial hyperreactivity: neural contributions. In: Kaliner MA and Barnes PJ (ed.) The airways. In: Lenfant C (ed.) Lung biology in health and disease. Marcel dekker, Inc. New York. Vol. 33. Pp 467–484

Cockcroft DW, Ruffin RE, Dolovich J, Hargreave FE (1977) Allergen–induced increase in non–allergic bronchial reactivity. Clin Allergy 7:503–13

Coyle AJ, Ackerman SJ and Irvin CG (1993a) Cationic proteins induce airway hyperresponsiveness dependent on charge interactions. Am Rev Respir Dis 147(4): 896–900

Coyle AJ, Mitzner W and Irvin CG (1993b) Cationic proteins alter smooth muscle function by an epithelium–dependent mechanism. J Appl Physiol 74(4): 1761–1768

Cutz E, Levison H and Cooper DM (1978) Ultrastructure of airways in children with asthma. Histopathology. 2: 407–421

Daniel EE and O'Byrne P (1991) Effect of inflammatory mediators on airway nerves and muscle. Am Rev Respir Dis 143(3 Pt 2): S3–5

Dillon PF Aksoy MO, Driska SP and Murphy RA (1981) Myosin physophorylation and the crossbridge cycle in arterial smooth muscle. Science Wash DC 211: 495–497

Ding DJ, Martin JG and Macklem PT (1987) Effects of lung volume on maximal methacholine–induced bronchoconstriction in normal humans. J Appl Physiol 62(3): 1324–30

Donnersberger AB (1980) A manual of anatomy and physiology: laboratory animal, the cat. 2nd ed. Heath: Lexington, Mass. Pp 283–298

Dunnill MS (1960) The pathology of asthma with special reference to changes in the bronchial mucosa. J Clin Pathol 13: 27–33

Dunnill MS (1964) Evaluation of a simple method of sampling the lung for quantitative histological analysis. Thorax. 19: 443

Dunnill MS, Massarella GR and Anderson LA (1969) A comparison of the quantitative anatomy of the bronchi in normal subjects, in status asthmaticus, in chronic bronchitis, and in emphysema. Thorax. 24: 176–179

Dunnill MS (1975) The morphology of the airways in bronchial asthma. In: New directions in asthma. ed. Myron Stein. The american college of chest physicians, Park Ridge, Illinois. Pp 213–221

Ebina M, Yaegashi H, Takahashi T, Motomiya M and Tanemura M (1990_a) Distribution of smooth muscle along the bronchial tree: A morphometric study of ordinary autopsy lungs. Am Rev Respir Dis 141: 1322–1326

Ebina M, Yaegashi H, Chiba R, Takahashi T, Motomiya M and Tanemura M (1990_b) Hyperreactive site in the airway tree of asthmatic patients revealed by thickening of bronchial muscles: A morphometric study. Am Rev Respir Dis 141: 1327–1332

Ebina M, Takahashi T, Chiba T and Motomiya M (1993) Cellular hypertrophy and hyperplasia of airway smooth muscle underlying bronchial asthma: a 3–D morphometric study. Am Rev Respir Dis 148:720–6

Elsen J and Arey LB (1966) On spirality in the intestinal wall. Am J Anat 118(1): 11–20

Fawcett DF (1986) Histology. 11th ed. Saunders Company, Philadelphia. Pp 735–742

Finlay HM (1989) Spatial orientation of arterial sections determined from aligned vascular smooth muscle. Journal of microscopy, Vol. 155: 215–226

Fiore MSH di (1989) Atlas of normal histology. 6th ed. Lea and Febiger, Philadelpha. Pp 60

Fraser RG, Pare JAP, Pare PD, Fraser RS and Genereux GP (1988) Diagnosis of diseases of the chest. 3nd ed. Saunders, Philadelphia. Pp 3–30

Fraser RS, Pare JAP, Fraser RG and Pare PD (1994) Synopsis of diseases of the chest. 2nd ed. Saunders, Philadelphia. Pp 365–369

Frigas E and Gleich GJ (1986) The eosinophil and the pathology of asthma. J Allergy Clin Immunol 77: 527–537

Gabella G (1973) Cellular structures and electro–physiological behaviour: fine structure of smooth muscle. Phil Trans R Soc Lond. B 265: 7–16

Gabella G (1981) Structure of smooth muscles. In: Bulbring E, Brading AF, Jones AW and Tomita T. Smooth muscle: an assessment of current knowledge. Edward Arnold Ltd, London. Pp 1–46

Ganong WF, Rudolph CD and Zimmermann H (1979) Neuroendocrine components in the regulation of blood pressure and renin secretion. Hypertension. 1(3): 207–218

Ganong WF (1991) Review of medical physiology. Chapter 3. Excitable tissue: muscle. 15th ed. Norwalk, Conn. Appleton & Lange. Pp 72–73

Gao Y and Vanhoutte PM (1994) Epithelium acts as a modulator and a diffusion barrier in the responses of canine airway smooth muscle. J Appl Physiol 76: 1843–1847

Hartshorne DJ (1987) Biochemistry of the contractile process in smooth muscle. In: Johnson LR (ed.) Physiology of the Gastrointestinal Tract. Raven Press, New York. Pp 423–482

Hayek H von (1960) The human lung. Hafner, New York. Pp 139–151

Hayward J and Reid L (1952_a) Observations on the anatomy of the intrasegmental bronchial tree. Thorax 7: 89–97

Hayward J and Reid L (1952_b) The cartilage of the intrapulmonary bronchi in normal lungs, in bronchiectasis and in massive collapse. Thorax 7: 98–110

Heard BE and Hossain S (1973) Hyperplasia of bronchial muscle in asthma. J Pathol 110: 319–31

Heumann HG (1970) A regular actin filament lattice in a vertebrate smooth muscle. Experientia 26:1131–1132

Hogg JC (1980) The respiratory airways. In Guenther CA and Welch MH (eds.). Pulmonary medicine. Philadelphia: Lippincott. Chap 3.

Hogg JC (1985) The pathology of asthma. In: Weiss EB, Segal MS and Stein M. BRONCHIAL ASTHMA: mechanisms and therapeutics. 2nd, ed. Little and Brown, Boston. Pp 209–217

Horsfield K (1974) The relation between structure and function in the airways of the lung. Br J Dis Chest 68: 145–60

Hudgel DW (1994) Bronchial asthma. In Baum GL and Wolinsky E. Pulmonary diseases. 5th Edition. Little, Brown and Company, New York. Pp 647–687

Jacoby DB, Ueki IF, Widdicombe JH, Loegering DA, Gleich GJ and Nadel JA (1988) Effect of human eosinophil major basic protein on ion transport in dog tracheal epithelium. Am Rev Respir Dis 137: 13–16

James AL, Pare PD and Hogg JC (1989) The Mechanics of airway narrowing in asthma. Am Rev Respir Dis 139: 242–246

Kaliner M (1989) Asthma and mast cell activation. J Allergy Clin Immunol. 83: 510–520

Kay AB (1985) Eosinophils and neutrophils in the pathogenesis of asthma. In: Weiss EB, Segal MS and Stein M. BRONCHIAL ASTHMA: mechanisms and therapeutics. 2nd, ed. Brown and Company, Boston. Pp 255–265

Kay AB, Henson PM, Hunninghake GW, Irvin C, Lichtenstein LM and Nadel JA (1989) Cellular mechanisms. In: Holgate ST et al. (ed). The role of inflammatory processes in airway hyperresponsiveness. Blackwell scientific publications, Oxford London. Pp 151–178

Kay AB, Ying S, Varney V, Gaga M, Durham SR, Moqbel R, Wardlaw AJ and Hamid Q (1991) Messenger RNA expression of the cytokine gene cluster, interleukin 3 (IL–3), IL–4, IL–5, and granulocyte/macrophage colony–stimulating factor, in allergen–induced late–phase cutaneous reactions in atopic subjects. J Exp Med 173:775–778

Kockx MM, Wuyts FL, Buyssens N, Van Den Bossche RM, De Meyer GR, Bult H and Herman AG (1993) Longitudinally orientated smooth muscle cells in rabbit arteries. Virchows Archiv A Pathol Anat 422: 293–299

Krause WJ and Cutts HJ (1981) Concise text of histology. Williams & Wilkins, Baltimore. Pp 128–129

Laitinen A and Laitinen LA (1994) Airway morphology: epithelium/basement membrane. Am Rev Respir Dis. 150(Suppl): S14–17

Laitinen LA, Heino M, Laitinen A, Kava T and Haahtela T (1985) Damage of the airway epithelium and bronchial reactivity in patients with asthma. Am Rev Respir Dis 131: 599–606

Laitinen L, Laitinen LA, Moss R and Widdicombe JG (1989) Organization and structure of the tracheal and bronchial blood vessels in the dog. J Anat. 165: 133–140

Lamb D (1990) Pathology (of asthma). Respiratory Medicine. London: Bailliere Tindall; Pp 603–609

Leeson CR (1976) Histology. 3d ed. Sanders, Philadelphia. Pp 182–184

Lopez–Vidriero MT, Bhaskar KR and Reid LM (1993) Bronchial mucus. In: Weiss EB and Stein M. Bronchial asthma: mechanisms and therapeutics. 3rd ed. Little, Brown and company Inc., New York. Pp 356–370

Macklin CC (1929) The musculature of the bronchi and lungs. Physiol Rev 9: 1–60

Matsuno T, Tokunaka S and Koyanagi T (1984) Muscular development in the urinary tract. Journal of Urology. 132(1): 148–52

McFadden ER Jr. (1988) Asthma: general features, pathologenesis, and pathophysiology. In Fishman AP. Pulmonary diseases and disorders. 2nd Edition. McGraw–Hill Book Company, New York. Pp 1295–1310

McKirdy HC and Macmillian J (1971) Spirality of the muscle layers of the intestine. Experientia. 27(7): 790

Miller WS (1937) The lung. Springfield, IL: Thomas. Pp 15–55

Milne A.A.Y. and Piper P.J. (1994) The effects of two anti–CD18 antibodies on antigen–induced airway hyperresponsiveness and leukocyte accumulation in the guinea pig. Am J Respir Cell Mol Biol Vol. 11. Pp 337–343

Montefort S and Holgate ST (1993_a) Bronchial epithelial shedding in asthmatics and non–asthmatics. Respiratory Medicine 87: (Suppl B) 9–11

Montefort S, Djukanovic R, Holgate ST and Roche WR (1993_b) Ciliated cell damage in the bronchial epithelium of asthmatics and non–asthmatics. Clinical & Experimental Allergy 23: 185–189

Moreno RH, Hogg JC and Pare PD (1986) Mechanics of airway narrowing. Am Rev Respir Dis 133: 1171–1180

Murray JF (1986) The normal lung: the basis for diagnosis and treatment of pulmonary disease. 2ed ed. Saunders, Philadelphia. Pp 33

Nagaishi C (1972) Functional anatomy and histology of the lung. University Park Press, Baltimore and London. Pp 7–9

Netter FH (1979) Respiratory system: a compilation of paintings depicting anatomy and embryology, physiology, pathology, pathophysiology, and clinical features and treatment of diseases. ed. Divertie MB and Brass A. The CIBA collection of medical illlustrations. Volume 7. Summit N.J. CIBA Pp 119–135

Newball HH and Lichtenstein LM (1981) Mast cell and basophils: effector cells of inflammatory disorders in the lung. Thorax 36: 721–5

Omari TI, Sparrow MP and Mitchell HW (1993) Responsiveness of human isolated bronchial segments and its relationship to epithelial loss. Br J clin Pharmac 35: 357–365

Opazo–Saez A, Okazawa M and Pare PD (1994) Airway smooth muscle orientation and airway stiffness favor airway narrowing rather airway shortening (abstract). Am Rev Respir Dis 149(4): A583.

Reed CE (1980) Asthma. In: Current pulmonology. Simmons DH ed. vol. 2, Houghton Mifflin, Boston. Pp 69–101

Rhodin JAG (1980) Architecture of the vessel wall. In: Handbook of Physiology. Bohr DF, Somlyo AP and Sparks HV. Am Physiol Soc 1980, Sect. 2, Vol. 2, Pp 1–32

Rice RV, Moses JA, McManus GM,Brady AC and Blasik LM (1970) The organization of contractile filaments in a mammalian smooth muscle. J Cell Biol 47: 183–196

Robinson DS, Hamid Q, Ying S, Tsicopoulos A, Barkans J, Bentley AM, Corrigan CC, Durham SR and Kay AB (1992) Predominant T_{H2}–like bronchoalveolar T–lymphocyte population in atopic asthma. N Engl J Med 320(5): 298–304

Roche WR, Beasley R, Williams J and Holgate ST (1989) Subepithelial fibrosis in bronchi of asthmatics. Lancet. i: 520–524

Rodger IW (1992) Airway smooth muscle. British Medical Bulletin. 48(1): 97–107

Roitt I, Brostoff J, Male D (1989) Hypersensitivity–Type I. In:Immunology. 2nd ed. Grower Medical Publishing, New York. Pp 19.1–19.20

Rosenzweig LJ (1993) Anatomy of the cat. Wm. C. Brown Publishers, Dubuque, Iowa. Pp 143–151

Ryan G, Dolovich MB, Roberts RS, Frith PA, Juniper EF, Hargreave FE and Newhouse MT (1981) Standardization of inhalation provocation tests: two techniques of aerosol generation and inhalation compared. Am Rev Respir Dis 123(2): 195–9

Saetta M, Di Stefano A, Rosina C, Thiene G and Fabbri LM (1991) Quantitative structural analysis of peripheral airways and arteries in sudden fatal asthma. Am Rev Respir Dis 143: 138–143

Shoenberg CF and Needham DM (1976) A study of the mechanism of contraction in vertebrate smooth muscle. Biol Rev 51: 53–104

Sparrow MP, Pfitzer G,Gagelmann M and Ruegg JC (1984) Effect of calmodulin, Ca^{2+}, and cATP protein kinase on skinned tracheal smooth muscle. Am J Physiol 246(Cell Physiol 15): C308–314

Spencer H (1984) Pathology of the lung. 4th ed. Pergamon press, Oxford, New York. Pp 32–35

Stephens NL, Meyers JL and Cherniack RM (1968) Oxygen, carbon dioxide, H^+ ion, and bronchial length–tension relationships. J Appl Physiol 25: 376–383 n

Stephens NL, Kroeger E and Mehta JA (1969) Force–velocity characteristics of airway smooth muscle. J Appl Physiol 26: 685–92 n

Stephens NL, Mitchell RW, Antonissen LA, Kromer U, Hanks B, Kroeger EA and Kepron W (1980_a) Airway smooth muscle: physical properties and metabolism. In: Hargreave FE. AIRWAY REACTIVITY: mechanisms and clinical relevance. Astra Phamaceuticals Canada Ltd, Pp 110–114

Stephens NL and Kroeger EA (1980_b) Ultrastructure, biophysics and biochemistry of airway smooth muscle. In: Nadel JA (ed.) Physiology and pharmacology of the airways. Marcel Dekker, New York. Pp 31–121

Stephens NL and Hoppin FG jr. (1986) Mechanical properties of airway smooth muscle. In: Handbook of Physiology. The Respiratory System. Mechanics of Breathing. Bethesda, MD: Am Physiol Soc, 1986, sect. 3, vol. III, Pp 263–276

Stephens NL (1987) State of art: airway smooth muscle. Am Rev Respir Dis 135: 960–975

Stephens NL, Kong SK and Seow CY (1988) Mechanisms of increased shortening of sensitized airway smooth muscle. In: Armour C, Black J and Anderson S (eds.) Mechanisms in asthma: pharmacology, physiology, and management. Alan R. Liss, New York. Pp 231–354

Stephens NL (1992) The biophysics and biochemistry of smooth muscle contraction. Can J Physiol Pharmacol 70: 515–31

Sterk PJ, Daniel EE, Zamel N and Hargreave FE (1985) Limited bronchoconstriction to methacholine using partial flow–volume curves in nonasthmatic subjects. Am Rev Respir Dis 132: 272–277

Sturgess JM (1977) The mucous lining of major bronchi in the rabbit lung. Am Rev Respir Dis 115: 819–827

Suzuki H, Morita K and Kuriyama H (1976) Innervation and properties of the smooth muscle of the dog trachea. Jpn J Physiol 26: 303–320

Tang DC, Stull Jt, Kubota Y and Kamm KE (1992) Regulation of the Ca^{2+} dependence of smooth muscle contraction. J Biol Chemistry 267: 11839–11845

Tani E, Yamagata S and Ito Y (1977) Cell membrane structure of vascular smooth muscle of circle of Willis. Cell Tiss Res 179: 131–142

Turner–Warwick M (1989) Asthma. In: Turner–warwick M, Hodson ME, Corrin B and Kerr IH. Respiratory diseases: clinical atlas. Lippincott: London gower medical publishing, Phyladelphia. Pp 15.2–15.16

van Breemen C, Aaronson P, Loutzenhiser R and Meisheri K (1980) Ca^{2+} movements in smooth muscle. Chest 78(1 Suppl): 157–165

Walmsley JG, Gore RW, Dacey RG Jr, Damon DN and Duling BR (1982) Quantitative morphology of arterioles from the hamster cheek pouch related to mechanical analysis. Microvascular research 24: 249–271

Wang J, Jiang H and Stephens HL (1994) A modified force–velocity equation for smooth muscle contraction. A Appl Physiol 76: 253–258

Wang NS (1988) Anatomy. In: Dail DH and Hammar SP. Pulmonary Pathology. Springer–Verlag, New York. Pp 17–39

Weibel ER (1963) Morphometry of the human lung. Academic press Inc. Spring-Verlag, New York. Pp 110-130

Weibel ER (1968) A note on lung fixation. Am Res Respir Dis 97: 463-465

West JB, Bhargava V and Goldberger AL (1986) Beyond the principle of similitude: renormalization in the bronchial tree. J Appl Physiol. 60(3): 1089-1097

Wiggs BR, Moreno R, Hogg JC, Hilliam C and Paré PD (1990) A model of the mechanics of airway narrowing. J Appl Physiol 69(3): 849-860

Wiggs BR, Moreno R, James A, Hogg JC and Paré PD (1991) A model of the mechanics of airway narrowing in asthma. In: Asthma: its pathology and treatment. ed. Kaliner MA and Barnes PJ. New Yoek: Dekker Pp73-101

Wiggs BR, Bosken C, Paré PD, James A and Hogg JC (1992) A model of airway narrowing in asthma and in chronic obstructive pulmonary disease. Am Rev Respir Dis 145: 1251-1258

Williams MH Jr. (1981) Why do the airway contain smooth muscle? Lung 159: 291-293

Wong AYK and Klassen GA (1993) A model of calcium regulation in smooth muscle cell. Cell Calcium 14: 227-243

Woolcock AJ, Salome CM and Yan K (1984) The shape of the dose-response curve to histamine in asthmatic and normal subjects. Am Rev Respir Dis 130: 71-75

Workshop Report: Workshop on airway smooth muscle. Am Rev Respir Dis 1985, 131: 159-162

Xu LJ, Dandurand RJ, Lei M and Eidelman DH (1993) Airway hyperresponsiveness in cigarette smoke-exposed rats. Lung 171: 95-107

Yeh HC, Schum GM and Duggan MT (1979) Anatomic models of the tracheobronchial and pulmonary regions of the rat. Anat Rec. 195: 483-492